



GEDEON RICHTER

Master's thesis

***In silico* modeling of cooperative ligand binding**

by

Márton Vass

MSc program in Chemistry

Supervisor:

Dr. György Keserű

Gedeon Richter Plc. Hungary

Co-supervisor:

Dr. András Perczel

ELTE TTK, Department of Organic Chemistry

Eötvös Loránd University, Faculty of Science

Department of Physical Chemistry

May 2011, Budapest, Hungary

Acknowledgements

In the first place I would like to express my gratitude to my supervisor, Dr. György Keserű, who made it possible for me to perform my thesis work at Gedeon Richter Plc. and introduced me to many aspects of pharmaceutical research. I also want to thank Mr. Keserű for the interesting research topic, his advice and constant flow of ideas concerning the work. I am also indebted to Ákos Tarcsay at Gedeon Richter Plc. for his guidance from the very first steps to the finishing touches of this thesis work. I am grateful for his help both in scientific and personal issues and for his assistance with the Schrödinger software. I also profited a great deal from discussions with Márk Sándor at Gedeon Richter Plc.

My parents deserve special mention for their constant support and interest in my work. The completion of this thesis would not have been possible without them. It's a delight that we can talk about Chemistry at the dinner table. Thanks to my little sister, who's not so little any more, for her caring and for tolerating my late-night stands. Thanks to all my friends and especially Bence Török for being there for me and for everyone else who somehow contributed to the writing of this thesis.

Table of contents

Introduction	1
Literature overview	3
Proteins exhibiting cooperative binding	3
Kinetic models of cooperative binding	7
Cooperativity in fragment based drug discovery	12
Determination of orthostericity	14
<i>In silico</i> prediction of cooperative binding	17
Molecular docking by Glide	21
Comparison to other docking tools	25
Methods	30
Assembly of data set	30
Structure preparation	31
Docking protocols	33
Results	35
Overall performance in binding mode reproduction	35
The effect of ligand number on docking performance	36
The effect of docking order on docking performance	38
Docking performance on the druglike subset	39
Docking performance on the closed site subset	40
Discussion	43
Case Studies	46
Cytochromes P450	46
HSP90 complexes with fragments	53
Conclusions	54
References	56
Appendix	62
English summary	64
Hungarian summary	65

Introduction

Cooperativity, defined in a very broad sense by the modulation of an interaction in the presence of another in the same system, is encountered on virtually all levels of biochemical complexity. Examples range from metal chelation through protein folding to communication between cells rendering cooperativity a powerful way of Nature to accelerate or regulate specific biological processes¹. This phenomenon can be brought about by two distinct mechanisms: either by structural reorganization upon the formation of the first interaction, generally referred to as allostery, or by pre-organization of several binding motifs, when after the first binding event the subsequent steps become intramolecular and thus usually enhanced.

The term allostery is most often used for binding of ligands to proteins at interaction sites far from the sites used by their natural substrates. However, there is also evidence in the literature of orthosteric modulation (i.e., ligands binding at the same site or binding region as the primary substrate). An allosteric modulator induces conformational changes in the protein that enhance or inhibit binding at the primary site. The mechanism of orthosteric modulation is not yet fully understood, though it is suggested that cooperativity in this case may not only manifest through structural reorganization of the enzyme but also through pushing and reorienting of the substrate by the effector ligand to a more productive conformation², alteration in solvation of the binding site³⁻⁵, effector induced change in the primary substrate's redox potential or through indirect steric effects on the reactive properties of potentially present cofactors or prosthetic groups of the enzyme^{6,7}.

If cooperativity plays a role in the catalytic activity of the enzyme under investigation, kinetics of the catalyzed reaction may differ qualitatively from the usual Michaelis-Menten profile. Examples of atypical kinetics include autoactivation detected as a sigmoidal dependence of the reaction rate on substrate concentration, heteroactivation, substrate inhibition and non-competitive inhibition⁸⁻¹⁰. Pharmaceutically relevant systems that frequently show such atypical kinetics include cytochromes P450^{11,12} (CYPs), among which a few isoforms (CYP3A4, CYP2D6, CYP2C9, CYP1A2, etc.) are responsible for the metabolism of the majority of marketed drugs¹³. Further such proteins are UDP-glucuronosyltransferases^{14,15} (UGTs) and glutathione S-transferases¹⁶ (GSTs) also involved in the metabolism of drugs and ATP-binding cassette (ABC) transporters¹⁷⁻²⁰ that are responsible for the translocation of various substances across the cell membrane. Representatives of this family are associated with multi-drug resistance in tumor cells and efflux of xenobiotics

typically in the blood-brain barrier. In these systems evidence has been brought forward by site-directed mutagenesis experiments²¹⁻²³, deuterium isotope effect experiments²⁴, NMR T₁ paramagnetic relaxation studies^{2,25-27} and the solution of protein-ligand complex structures by X-ray crystallography^{28,29} that the binding of the substrate and effector compounds happen at the same site or at sites close to each other. Recently published structures of CYP3A4 with two ketoconazole molecules bound³⁰ and mouse P-glycoprotein with two cyclic peptide inhibitors bound³¹ provided remarkable advances in the field. Homotropic cooperativity in metabolism results in increased clearance of drugs¹⁴, while heterotropic cooperativity may lie in the background of drug-drug interactions mediated by the aforementioned enzymes *in vivo*³²⁻³⁵. Computational prediction of cooperative binding of ligands could have great impact on lead optimization as it would help to sort out drug candidates with poor pharmacokinetic parameters and reduce the number and cost of experiments required in testing them.

The second mechanism leading to cooperativity is pre-organizing binding motifs to enhance binding affinity. The introduction of new functional groups in a molecule has both an enthalpic contribution to the affinity and an entropic one, since only a smaller fraction of the translational, rotational and conformational space needs to be sampled upon binding. The chemical space relevant in drug design can be more efficiently probed using fragments than by screening druglike molecules and hits can then be evolved into leads in several ways. These include growing by substitution at one or more positions to exploit additional possible protein-ligand interactions and linking two fragments binding to different but close regions of the protein with a suitable linker that lets the fragments retain their original binding conformations³⁶. The linking approach has also been implemented *in situ* by using fragments with reactive functional groups that give druglike compounds inside the binding site with good complementarity to the protein surface.

An efficient method to identify fragments suitable for linking has been described, in which a fragment hit from a first screen is added to the protein in high concentration so that it occupies the primary binding site and a second-site screen is performed to obtain proximally bound fragments. A subnanomolar inhibitor of Bcl-X_L³⁷ and a low micromolar inhibitor of HSP90³⁸ are published examples of the successful application of this approach. A similar method – in theory – could be implemented in a computational setup as well. Molecular docking could be used to identify first-site hits from a virtual fragment library then docking another library into the obtained protein-ligand complexes would result in hits binding to the

second site. Finding a suitable linker and finally docking the resulting compound as a whole to the receptor would then give advanced hits.

Given the two related areas of metabolic activation and fragment based approaches where cooperative ligand binding plays an important role we set out to investigate this phenomenon in a more general context by means of a computational approach. In the present study we aimed at exploring the possibilities of multiple molecular docking in reproducing cooperative binding conformations of ligands. A set of 115 X-ray crystal structures was collected from the RCSB Protein Data Bank (PDB) containing at least two non-cofactor type ligands in close proximity to each other believed to be a result of cooperative binding. The commercial docking software Glide was used to perform sequential docking of the ligands to their respective structures in a self-docking setup and the performance of the method was then analyzed. There has been debate about the accuracy of scoring functions for fragment binding modes though a recent study on 190 protein-fragment complexes³⁹ showed that Glide is adequate for fragment docking even in cross-docking setups. Thus the pharmaceutically relevant subset of cytochrome P450 enzymes and results of structures from fragment screens were further investigated.

Literature overview

Proteins exhibiting cooperative binding

The appearance of orthosteric cooperativity requires the binding of two or more ligands in a single binding site of the protein. Since specific enzymes usually accommodate only one copy of their substrate in an active site specifically designed for that ligand it is not surprising that orthosteric binding is most often observed in promiscuous proteins with larger binding sites. While there is a limited, though large number of endogenous compounds enzymes need to recognize, xenobiotics can comprise virtually any structural feature. Thus proteins involved in the manipulation of these compounds, e.g. metabolic enzymes and transporters, tend to have large and aspecific binding sites prone to orthosteric binding of multiple ligands. Metabolism of xenobiotics usually involves two phases: in phase I polar groups are introduced into the mostly lipophilic molecules by oxidation, reduction or hydrolysis and in phase II they are conjugated with polar endogenous compounds (glucuronic acid, glutathione,

amino acids, sulfate or acetyl groups). The resulting water soluble products are finally excreted.

Enzymes belonging to the cytochrome P450 superfamily contain a heme prosthetic group anchored by a cysteine residue coordinated to the iron atom and are involved in the transformation of both endogenous and xenobiotic compounds in bacteria, fungi, plants and animals¹¹⁻¹³. Eukaryotic CYPs are membrane bound thus their crystallization has only recently been accomplished. In humans 57 isoforms can be found responsible for the biosynthesis of steroids and the phase I metabolism of fatty acids and xenobiotics. Mammalian CYP families are characterized by > 40 % amino acid identity and designated by Arabic numerals, subfamilies share > 55 % amino acid identity and are designated by capital letters, while individual isoforms are indicated by another numeral.

The catalytic cycle of CYP enzymes was elucidated based on experiments with the bacterial camphor monooxygenase (CYPcam or CYP101). When a substrate molecule (RH) displaces the water coordinated to the iron atom a series of two one-electron reduction steps by NADPH-P450 reductase, O₂ coordination to the heme, protonation and water elimination steps are initiated resulting in the formation of the catalytically active ferryl-oxo species. It formally contains Fe(IV) and has a radical cationic character on the porphyrin moiety, which makes it a powerful electron acceptor. It can abstract an electron even from saturated hydrocarbons and form an iron-hydroxo species and an alkyl radical through a Fe—O···H···R transition state. The alkyl radical then also binds to the oxygen forming an alcohol (ROH) as a product coordinated to the iron. If the carbon involved in the hydrogen abstraction reaction is bound to a heteroatom, the product is spontaneously cleaved after dissociation from the binding site resulting formally in heteroatom dealkylation. If the electron is abstracted from an unsaturated compound, the rebinding of the radical results in an epoxide coordinated to the iron, which may rearrange nonenzymatically to a phenol for aromatic compounds. Furthermore *N*- or *S*-oxidation and several other metabolic reactions were also observed with CYPs. The isoforms CYP3A4, CYP2D6, CYP2C9, CYP2C19 and CYP1A2 are responsible for the metabolism of ~70 % of marketed drugs. Representative metabolic reactions mediated by CYP3A4 are shown in Figure 1.

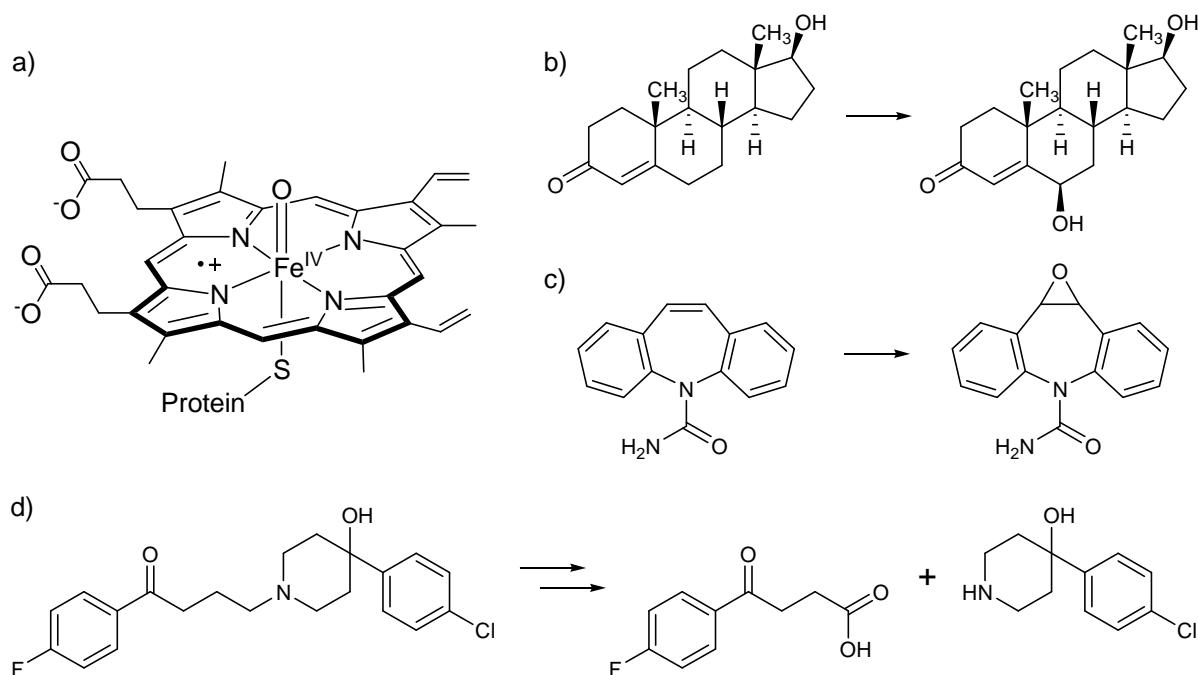


Figure 1. Representative metabolic reactions mediated by CYP3A4 a) the catalytically active ferryl-oxo species of cytochromes P450 b) testosterone 6 β -hydroxylation c) carbamazepine-10,11-epoxidation d) haloperidol *N*-dealkylation.

UDP-glucuronosyltransferases (UGTs) and glutathione *S*-transferases (GSTs) are phase II metabolic enzymes catalyzing the conjugation of endogenous substrates and xenobiotics with the carbohydrate glucuronic acid and the tripeptide glutathione, respectively¹⁴⁻¹⁶. Conjugation happens at a hydroxyl, thiol, amino or carboxyl group of the substrate, either originally present or introduced in phase I metabolism. Endogenous substrates of UGTs include bilirubin, steroid hormones, fatty acids, bile acids and retinoids. Direct glucuronidation is the primary metabolic pathway for ~15 % of marketed drugs though it is encountered frequently as a secondary metabolic mechanism. GSTs are dimeric enzymes present mostly in the cytosol. Glutathione serves also as an antioxidant and may react with xenobiotics to some extent even without the catalytic activity of GST enzymes. Though kinetic profiles indicative of cooperative binding have been reported for both enzyme families, the mechanisms of their activities so far remain poorly understood.

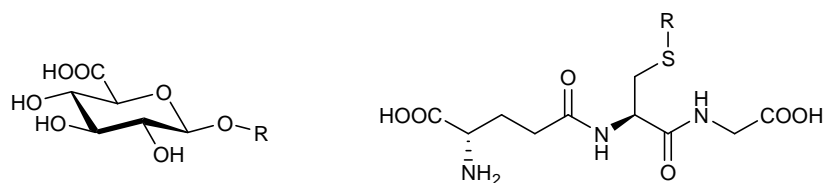


Figure 2. The structure of glucuronide (left) and glutathione conjugates (right).

ATP-binding cassette (ABC) transporters are one of the most ancient enzyme family found in all species responsible mainly for the efflux of various substances through the cell membrane but also involved in translation and DNA repair¹⁷⁻²⁰. They are large (~60-220 kDa) proteins consisting of two transmembrane domains (TMD) generally of 6-6 α -helices with variable architecture and two highly conserved cytoplasmic nucleotide binding domains (NBD). The helices form a chamber in the membrane open intracellularly in the resting state of the protein. The substrate enters this chamber from the inner leaflet of the lipid bilayer inducing a conformational change in the NBDs, which increases their affinity for ATP. The binding of two ATP molecules then brings about the formation of a closed NBD dimer, which in turn induces conformational changes in the TMDs. The chamber opens in the opposite direction and the binding affinity of the substrate decreases resulting in its ejection to the extracellular space. Finally hydrolysis of ATP and release of P_i and ADP restores the starting configuration of the transporter (see Figure 3). Mammalian P-glycoprotein (ABCB1) is the best characterized of all ABC transporters, though only a pair of low-resolution crystal structures is yet available due to difficulties in crystallization. It is a major constituent in the defense mechanism against xenobiotics in the blood-brain barrier and its overexpression in cancer cells leads to resistance to a variety of chemotherapeutic drugs. Its substrates are mostly lipophilic and either cationic or neutral but otherwise structurally very diverse. Promiscuity of this enzyme and observed multiple substrate binding can again be attributed to the large and mostly hydrophobic active site.

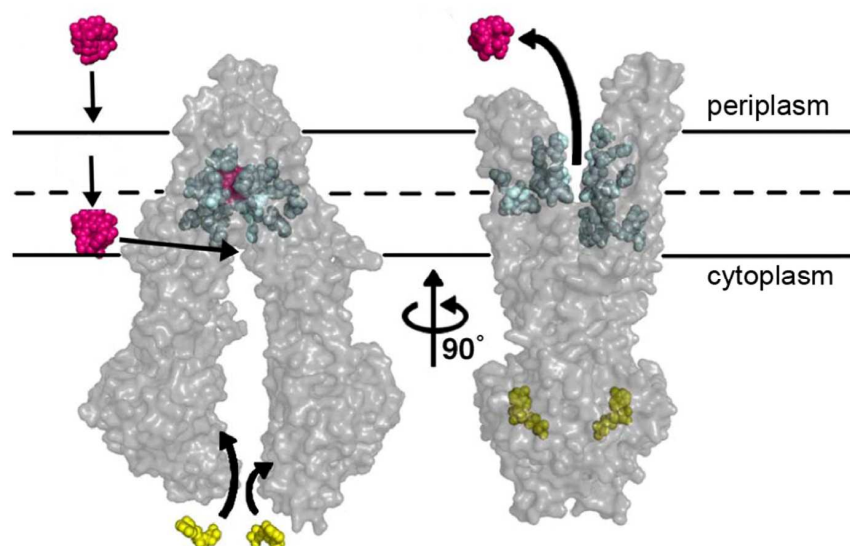
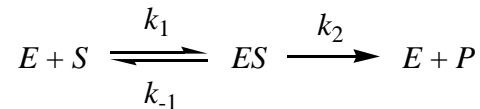


Figure 3. Mechanism of substrate transport by P-glycoprotein. Substrate is colored magenta, ATP yellow and active site residues cyan. Horizontal lines indicate the lipid bilayer of the cell membrane. Figure is reproduced from ref. 31.

Kinetic models of cooperative binding

Classic kinetic treatment of enzymatic reactions involves the utilization of the Michaelis-Menten model. This model assumes a reversible binding step of a single substrate (S) molecule to the enzyme (E) and an irreversible product formation step with the product (P) rapidly dissociating from the binding site:



Using the steady-state approximation for the concentration of the enzyme-substrate complex and assuming that the total enzyme concentration does not change in the course of the reaction one gets the well-known formula relating the rate of product formation to the concentration of the substrate:

$$\frac{d[P]}{dt} = v = k_2[E]_{TOT} \frac{[S]}{\frac{k_{-1} + k_2}{k_1} + [S]} = \frac{v_{max}[S]}{K_M + [S]}$$

where v_{max} is the maximal reaction rate at saturating substrate concentrations and K_M is the Michaelis constant. This model thus describes a hyperbolic dependence of the rate of product formation on the concentration of the substrate.

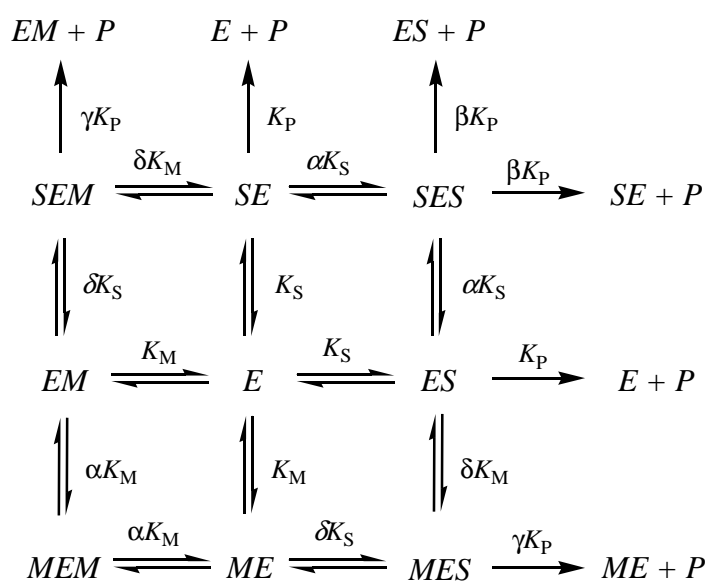
The first modification to the Michaelis-Menten model for describing multiple substrate binding was proposed by Hill in 1910 in an attempt to explain the sigmoidal binding curves of O_2 to hemoglobin⁴⁰. The Hill model assumes infinite cooperativity between multiple binding events, i.e. the simultaneous binding of all ligands to the enzyme. The rate formula derived from this assumption is suitable for the analysis of processes exhibiting a high degree of cooperativity:

$$v = \frac{v_{max}[S]^n}{K' + [S]^n}$$

where n is the Hill coefficient, which is less than or equal (in the limiting case of infinite cooperativity) to the number of binding sites and K' is the apparent dissociation constant of ES_n . The Hill model is still used in radioligand drug-binding and drug-transport measurements of ABC transporters with v_{max} there representing the maximal transport rate or maximal binding instead of maximal product formation rate. However, this formula did not give

satisfactory fits to kinetic curves of metabolite formation in CYP and UGT mediated metabolic reactions and it could not account for heterotropic effects, therefore a more sophisticated two-site mechanistic model was derived by Korzekwa et al. in 1998.⁴¹ This model was later extended⁸⁻¹⁰ and the generalized version is presently used in studies analyzing CYP and UGT mediated metabolism kinetics.

This mechanistic model comprises two similar binding sites, both of which can accommodate either a substrate or a modifier (*M*) molecule and these binding steps are all reversible. It is assumed that only the substrate is metabolized and product is irreversibly formed from the substrate regardless of which binding site it occupies and whether the modifier is also bound to the enzyme. A set of parameters are introduced to account for cooperativity. These are scaling factors of the dissociation constants and product formation rate coefficients of doubly versus singly ligated structures. The model is described by the following scheme:



where K_S and K_M are the dissociation constants of the enzyme-substrate and enzyme-modifier complexes respectively, K_P is the rate coefficient of product formation, α is the scaling factor of the dissociation constant of the second bound compound in the homotropic case, β is the scaling factor of the rate of product formation in the homotropic case, while δ and γ are similar scaling factors for heterotropic binding. A significant advantage of the model over the Hill formula is that it allows the simultaneous fit of the data covering the full range of modifier concentrations, while a different Hill coefficient was formerly obtained for each specific concentration. Also this mechanistic model can be arbitrarily simplified or refined

depending on the features of the observed kinetic curves and the number and precision of available data points. Using the same approximations as in the Michaelis-Menten model the formula obtained for the reaction rate is:

$$\frac{v}{v_{max}} = \frac{\frac{[S]}{K_S} + \frac{\beta[S]^2}{\alpha K_S^2} + \frac{\gamma[S][M]}{\delta K_S K_M}}{1 + \frac{2[S]}{K_S} + \frac{[S]^2}{\alpha K_S^2} + \frac{2[S][M]}{\delta K_S K_M} + \frac{2[M]}{K_M} + \frac{[M]^2}{\alpha K_M^2}}$$

When considering only homotropic effects concentration of the modifier is set to zero and the formula reduces to a quadratic fractional expression in $[S]$. The Michaelis-Menten equation is then a special case with $\alpha = \beta = 1$. Within the scope of this kinetic model autoactivation is characterized either by increased binding affinity of the second substrate (the dissociation constant is decreased by the scaling factor $\alpha < 1$) or by increased product formation rate from the double occupancy complex (scaling factor $\beta > 1$). These effects result in sigmoidal dependence of the reaction rate on substrate concentration. When $\beta < 1/2$ the formula describes the case of substrate inhibition, which is detected in kinetic measurements as a decrease in the rate of product formation once a specific concentration of the substrate is surpassed. When the binding affinity of the second substrate and the product formation rate from the *SES* complex change in opposite directions there is still a chance of observing autoactivation if $\beta > 1/2$ and $\alpha < \beta/2$ but when the parameters do not fall in either this range or that of substrate inhibition the resulting curve can be virtually undistinguishable from a hyperbolic one. Thus in theory it is possible that multiple substrate molecules are bound to the enzyme yet the observed kinetic profile suggests single binding.

Sigmoidicity is not always obvious on first inspection of the data as it is relevant only at the low end of substrate concentrations therefore Eadie-Hofstee and clearance plots are commonly used as diagnostic indicators of cooperative binding. Eadie-Hofstee plots are obtained by plotting the product formation rate against clearance, which results in a linear graph for the Michaelis-Menten model but the graph has a curvature when either type of cooperative binding is present. Clearance is the ratio of the reaction rate and substrate concentration in *in vitro* experiments. A clearance plot is a semi-logarithmic plot of clearance against substrate concentration, which is a monotonically decreasing function for single substrate binding or substrate inhibition but possesses a maximum when autoactivation is encountered. Representative plots are shown in Figure 4. The most notable shortcoming of the Hill model is its lack of ability to reproduce the low substrate concentration part of the

measured clearance profiles since the graph obtained from the Hill equation approaches zero at this range of concentrations. Thus if sufficient data points are available the inspection of these three diagrams allow the assignment of a suitable kinetic model to the reaction.

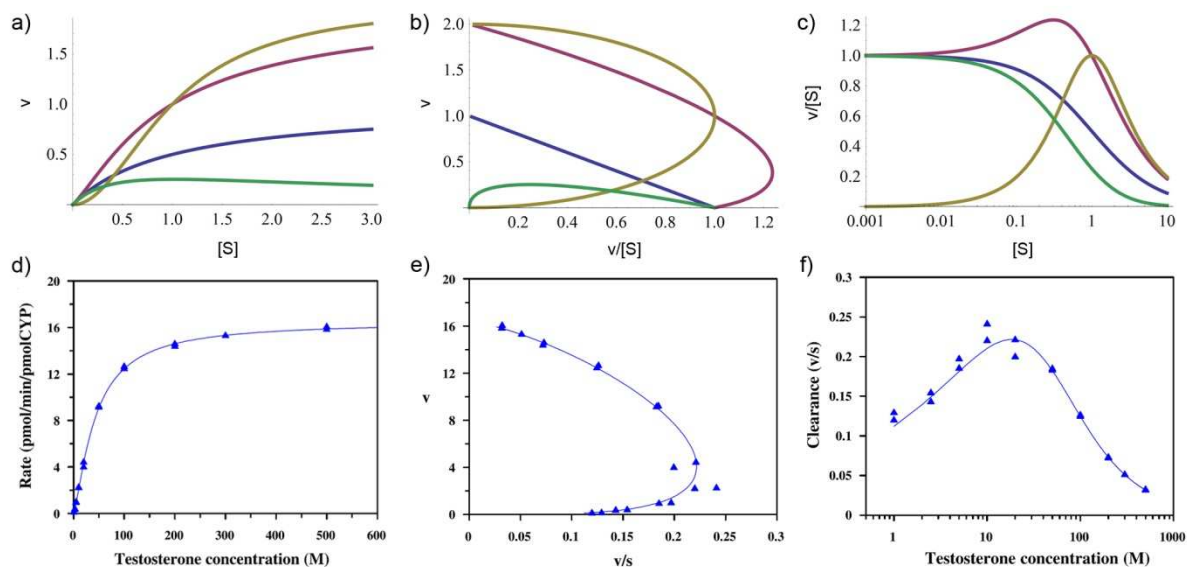


Figure 4. Theoretical and experimental kinetic curves for cooperative binding. a) Reaction rate plots for the Michaelis-Menten model with $v_{\max} = 1$, $K_M = 1$ (blue), the Hill model with $v_{\max} = 2$, $K' = 1$, $n = 2$ (yellow), the mechanistic model of autoactivation with $v_{\max} = 1$, $K_S = 1$, $\alpha = 0.5$, $\beta = 2$ (purple) and the mechanistic model of substrate inhibition with $v_{\max} = 1$, $K_S = 1$, $\alpha = 1$, $\beta = 0.01$ (green). b) Eadie-Hofstee plots for the same models. c) Clearance plots for the same models. d) Experimental reaction rate plot of CYP3A4 mediated testosterone 6β -hydroxylation. e) Experimental Eadie-Hofstee plot of the same reaction. f) Experimental clearance plot of the same reaction. Figures d), e) and f) are reproduced from ref. 9.

Heterotropic cooperative effects are only accounted for in the mechanistic kinetic model. Modifiers can be either activators when the rate of product formation increases with increasing concentrations of the modifier or inhibitors when the reaction rate decreases with increasing modifier concentrations. Heteroactivation manifests in a scaling factor of $\gamma > 1$, which means that product formation is enhanced when both substrate and modifier are bound to the enzyme, while inhibition is indicated by a $\gamma < 1$ value. In addition two different cases within inhibition can be distinguished based on the value of the δ parameter. A factor of $\delta < 1$ indicates cooperative inhibition i.e. increasing inhibitory effect with increasing concentrations of the modifier because the enzyme-substrate-inhibitor complex is more stable than the enzyme-substrate complex but the product formation rate from the former is lower than from the latter. The other case with opposite effects originating from the relative stabilities of the

complexes and relative product formation rates is termed partial inhibition ($\gamma < 1$, $\delta > 1$) since complete inhibition is not achieved even at saturating concentrations of the modifier. Representative plots for these cases and fits to experimental data are shown in figure 5.

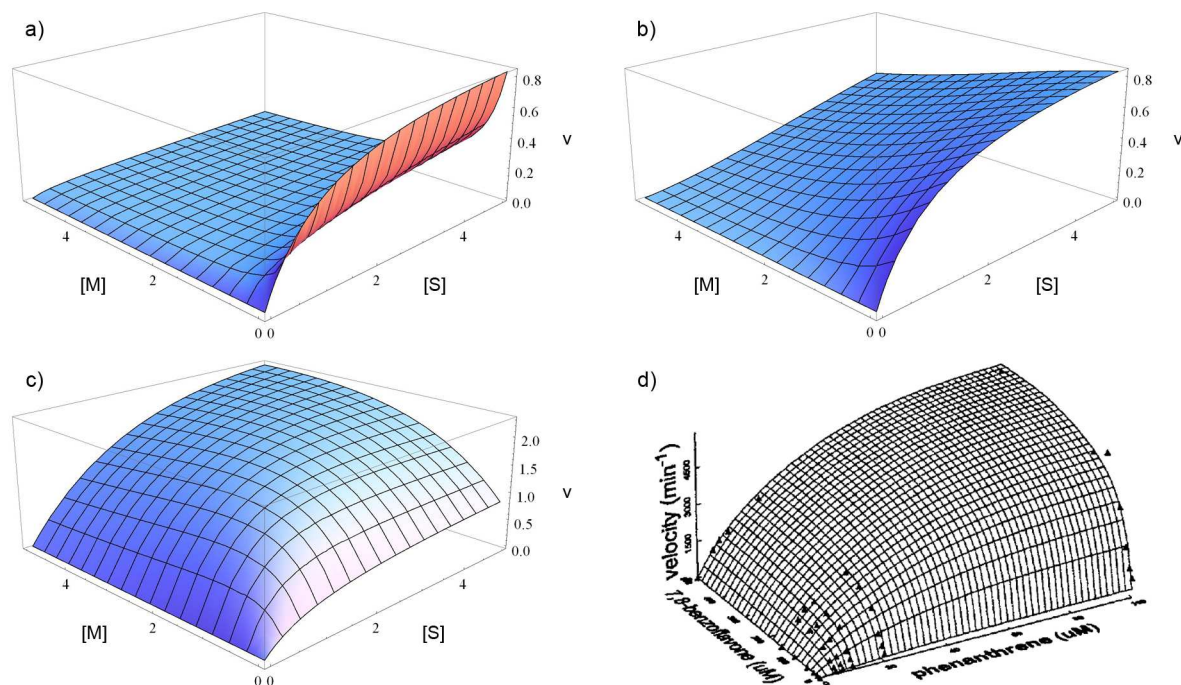


Figure 5. Theoretical and experimental kinetic profiles for heterotropic cooperative binding. $K_S = K_M = \alpha = \beta = 1$ for all theoretical plots. a) Cooperative inhibition with $\gamma = 0.1$, $\delta = 0.1$ b) Partial inhibition with $\gamma = 0.1$, $\delta = 10$ c) Heteroactivation with $\gamma = 10$, $\delta = 1$ d) Experimental reaction rate plot of CYP3A4 mediated phenanthrene 9,10-epoxidation activated by 7,8-benzoflavone. Figure d) is reproduced from ref. 41.

The two-site model predicts that close to saturating modifier concentrations even substrates otherwise exhibiting sigmoidal kinetic profiles revert to producing hyperbolic product formation rate plots. The reason for this is that at high modifier concentrations at least one of the binding sites is always occupied by the modifier and thus the system formally acts as an enzyme with a single site. However, there are reported cases of substrates retaining sigmoidal kinetic profiles even at high concentrations of a modifier. This phenomenon can only be explained by assuming the existence of more than two binding sites. The two-site mechanistic model is therefore augmented by a third site in several publications, which is usually assumed to bind only the modifier but the potential for generalization remains. Examples of substrates and modifiers of CYP3A4 metabolism exhibiting homotropic and heterotropic cooperativity are collected in Table 1.

kinetic profile with CYP3A4	examples
hyperbolic	midazolam, felodipine
autoactivation	testosterone, diazepam
substrate inhibition	nifedipine
heterotropic activation with S showing hyperbolic kinetics	quinidine effect on felodipine and simvastatin
partial inhibition with S showing hyperbolic kinetics	nifedipine effect on felodipine
cooperative inhibition with S showing hyperbolic kinetics	haloperidol effect on felodipine and quinidine
heterotropic activation with S showing sigmoidal kinetics	testosterone effect on diazepam
partial inhibition with S showing sigmoidal kinetics	haloperidol effect on testosterone
cooperative inhibition with S showing sigmoidal kinetics	quinidine and diazepam effect on testosterone

Table 1. Examples of different kinetic profiles observed in CYP3A4 mediated metabolic reactions: diazepam 3-hydroxylation, felodipine aromatization, haloperidol dealkylation, midazolam 1'-hydroxylation, nifedipine aromatization, quinidine 3-S-hydroxylation, simvastatin 3'-hydroxylation, testosterone 6 β -hydroxylation. Data taken from ref. 42.

Cooperativity in fragment based drug discovery

Fragment based methods have recently gained attention in drug discovery and become recognized as alternatives to more widely used hit identification methods such as high throughput screening (HTS) and traditional medicinal chemistry³⁶. Fragments are low molecular weight polar compounds (typically < 250-300 Da) that comprise only a few structural features. These molecules bind with lower affinity to receptors, frequently in the micromolar to millimolar instead of nanomolar range. However, it is assumed that ligand efficiencies (binding free energy divided by the number of heavy atoms) are comparable or even higher than for druglike compounds. Because of the low binding affinity sensitive biophysical methods are typically needed to detect binding events and the recent development in such technologies made fragment based approaches amenable to practical use. Techniques employed in fragment screens are NMR spectroscopy, X-ray crystallography, surface plasmon resonance (SPR), mass spectrometry (MS) and isothermal titration calorimetry (ITC). The importance of using fragments instead of druglike compounds is that chemical space can be more efficiently sampled with them. The number of potential fragments has been estimated 10⁷, while the number of druglike molecules is considered to be around 10⁶⁰. Thus a fragment screen probing several thousands of molecules covers a much higher fraction of

possible structures than a traditional HTS experiment with even hundreds of thousands of molecules. Further advantages of these methods are the higher speed, lower cost and lower susceptibility to errors due to ligand solubility. Two main approaches are used in fragment to lead optimization. In the growing approach new groups are introduced into the single fragment hit to exploit additional protein-ligand interactions. A requirement for success is that the fragment does not change its binding mode during the optimization procedure. The linking approach on the other hand relies on the identification of two adjacently bound hits and a higher affinity compound is obtained by introducing a suitable linker between the two fragments either preparatively or in situ.

An example of the successful application of the linking method is the novel HSP90 inhibitor identified by Abbott Laboratories where the cooperative nature of binding was also assessed³⁸. In the first step of the procedure a fragment library of 11,520 compounds with average molecular weight of 225 Da was screened against the N-terminal domain of HSP90. Hits were identified by changes in chemical shifts of active site leucine, valine, and isoleucine methyl groups in two-dimensional ¹H/¹³C heteronuclear single quantum correlation (2D HSQC) NMR experiments. A complementary fluorescence resonance energy transfer (FRET) assay was also performed. A series of aminotriazine and a series of aminopyrimidine compounds were found to bind efficiently, a trifluoromethyl substituent bearing representative of the latter group exhibiting the highest ligand efficiency and a dissociation constant of 20 μ M. A second-site screen was performed by 2D NMR in the presence of saturating concentrations of this compound using a library of 3,360 compounds with average molecular weight of 150 Da. The most potent hit was 3-(anilinomethylene)-dihydrofuran-2-one binding to the protein with a dissociation constant of 150 μ M in the presence and > 5 mM in the absence of the first-site ligand. This indicates a strong cooperativity in the binding of the two ligands. In order to guide the linking strategy the ternary complex structure of the protein with the two hits was solved. A perpendicular orientation with a π - π stacking interaction between the ligands was observed, which indicated the need for a linker able to bend 180°. A methylsulfonamide moiety was suggested to be suitable for this purpose and the generated compound yielded a 10-fold improvement in potency relative to the first-site hit. The X-ray structure of HSP90 with the obtained ligand confirmed that the orientations of the two parts of the ligand were the same as in the ternary complex. A rough estimation employed by the authors suggested that for an optimal linker a dissociation constant of 30 nM could have been expected and the suboptimal result was attributed to the limited number of linkers evaluated.

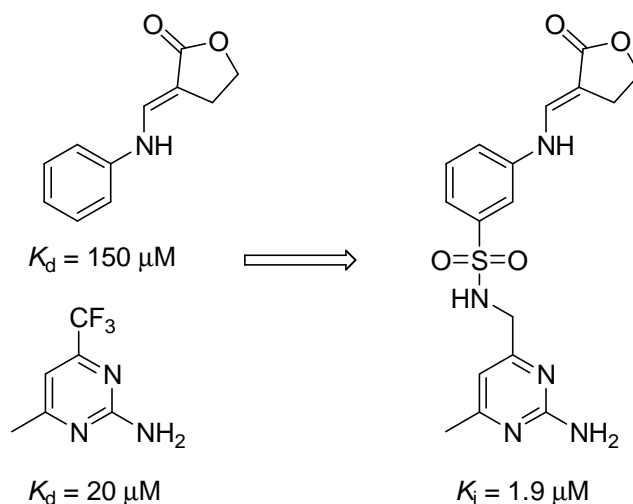


Figure 6. The linking strategy applied in the fragment based inhibitor design of HSP90.

Determination of orthostericity

Today high-resolution X-ray crystallography is the most reliable source of structural information on protein-ligand complexes. It provides unambiguous evidence for the orthosteric or allosteric nature of multiple ligand binding, though the relevance of higher stoichiometry complexes has to be confirmed by a different experimental method to rule out the possibility of binding as a crystallization artifact. Difficulties in the crystallization of proteins exhibiting cooperative binding have long denied insight into the structural features of this phenomenon. However, the emergence of several multiply ligated complex structures in the past ten years shows that these difficulties are slowly overcome^{28-31,72-77}. The primary information obtained from X-ray crystallography is the electron density map of the unit cell of the crystal and a model of the protein has to be built, which conforms to the observed electron densities. The unit cell may contain more than one copies of the macromolecule or the protein may have symmetry equivalent elements (e.g. in homo-oligomers) that produce crystallographic symmetry in the crystal. Therefore the biological assembly has to be assigned independently of the unit cell. Observed average electron densities of the ligands may be lower than those of the macromolecule if the ligand is not bound to all of the protein molecules contained in the crystal. This may be the case for low affinity ligands even in co-crystallization experiments but is usually relevant if the complex crystal is prepared by soaking the protein crystal in the ligand solution. After model building and structure refinement the atomic coordinates in the unit cell and B-factors are obtained. The B-factor is

proportional to the square of the average atomic displacement due to vibration for a perfect crystal but may be increased by disorders in the crystal or lower occupancy of the atoms. There are a variety of indicators used for describing the quality of the solved structure. The most common of them is undoubtedly the resolution, which is the minimal distance between crystal planes from which reflections could be observed. A resolution lower than 1 Å indicates atomic resolution, rotamers of side chains are usually correct under 2 Å, the protein fold is usually correct under 3 Å and individual atomic coordinates are meaningless above 4 Å. The error of atomic coordinates is not equal to the resolution, though correlates with it. They can be determined exactly in small molecule crystallography but can only be estimated for macromolecules by the use of Luzzati plots. Average coordinate errors for a well-refined structure are 0.2-0.3 Å. Another frequently used indicator of quality is the R-factor, which is the ratio of the difference between measured and calculated structure factors to the measured structure factors. A value lower than 0.2 is considered to be optimal. Recently also the free R-factor is reported for new structures, which is calculated in the same way but using only a small set of randomly chosen intensities that are not used during refinement. There should not be a difference greater than 0.05 between R and R_{free} . The completeness and redundancy of the data set also provide information about the quality of the measurement.

NMR based structure determination using Nuclear Overhauser Effect Spectroscopy (NOESY) may also be used to obtain information about the relative position and orientation of the ligands. This method has been used in fragment based drug discovery^{37,38}. Since NOE signals can usually be detected between protons not farther than 5-6 Å from each other, interligand dipolar couplings are usually not observed. Rather, the structure of the complex is obtained by docking the ligands to the binding site using protein-ligand intermolecular NOE signals as constraints.

In addition to X-ray crystallography and NOESY a few other methods assessing multiple ligand binding have been described, which do not rely on the full determination of the complex structure. Site-directed mutagenesis experiments had been performed by Halpert and co-workers on CYP3A4 before an X-ray structure of the protein became available^{21,22}. They identified active site amino acids to mutate employing homology modeling and used the metabolic reactions of testosterone, progesterone, α -naphthoflavone and 7-benzyloxy-4-(trifluoromethyl)coumarin to compare the activities of the wild-type enzyme and mutants. Many of the mutants displayed either a minor effect on metabolism or decreased reaction rates but the L210F (i.e. leucine 210 mutated to phenylalanine), L211F, F213W, D214E, and

I301F mutants displayed increased rates of metabolite formation while homotropic cooperativity present in the wild-type enzyme disappeared in these mutants. These findings implicated that the larger amino acids partially occupy the binding site of the effector but not that of the metabolized substrate. Based on the positions of these amino acids in the homology model the effector site was inferred to lie adjacent to the primary binding site.

Deuterium isotope effect experiments that utilize symmetrical and selectively labeled substrates were used to study substrate dynamics in CYP2A6 by Harrelson et al.²⁴ The $(k_H/k_D)_{\text{obs}}$ for the oxidation of these types of substrates reflects the rate of reorientation of the labeled and unlabeled sites on the substrate. For a rapidly reorienting substrate this ratio is the intrinsic isotope effect (~ 11.5 for d_3 -xylenes), while for slow reorientation it is 1. However, if there is an alternative non-labeled metabolic site on the substrate, metabolic switching may also affect the $(k_H/k_D)_{\text{obs}}$ ratio. If a second molecule of the substrate binds in the active site both the reorientation rate and the metabolic switching may change in a concentration-dependent manner due to steric crowding. Using m -xylene- α - $^2\text{H}_3$ the $(k_H/k_D)_{\text{obs}}$ did not change with concentration but a decrease in the m -methylbenzylalcohol : 2,4-dimethylphenol product ratio was observed, which implicated a decrease in reorientation rate and multiple substrate binding in the active site.

The presence of the paramagnetic iron center in CYPs permits the use of NMR Paramagnetic Relaxation Enhancement (PRE) for the determination of distances between ligand protons and the iron atom. PRE is a complementary technique to NOESY providing information on long-range distances typically up to 25 Å. It is based on the phenomenon of reduction of spin-lattice relaxation times (T_1) in the vicinity of unpaired electrons quantified by the Solomon-Bloembergen equation. The dependence of relaxation rates on internuclear distances is sixth order thus measured values are not true averages, rather describe the closest approach of a given proton to the heme iron. Paramagnetic T_1 values are measured with a simple inversion-recovery pulse sequence relative to a reference diamagnetic system (sodium-dithionite-reduced carbon monoxide complex of CYPs). Additionally dissociation constants of protein-ligand complexes need to be taken from kinetic measurements. Ligand proton – heme iron distances were determined using this method in ternary complexes of CYP2C9-flurbiprofen-dapsone², CYP3A4-midazolam- α -naphthoflavone²⁶, CYP3A4-midazolam-testosterone²⁶ and CYP3A4-acetaminophen-caffeine²⁷. Values ranging from 3 to 10 Å for both ligands in all complexes indicate their closeness to the heme iron, which can be realized only if the ligands are in close proximity to each other as well.

Fluorescent resonance energy transfer (FRET) can be used to measure distances up to 100 Å in proteins using suitably selected fluorescent labels and/or substrates. In these experiments the donor chromophore is excited, which transfers energy to the acceptor chromophore through nonradiative dipole-dipole coupling and the emission of the latter is measured. FRET efficiency depends on the distance and relative orientation of the two dipoles and the spectral overlap between the donor emission and the acceptor absorption spectrum. It is measured as $1 - \frac{\text{quantum yield of donor in presence of acceptor}}{\text{quantum yield of donor in absence of acceptor}}$. Dependence on the distance is sixth order as in PRE. Though this method has not been directly used to measure distances between two ligands bound to a single protein, the distance of P-glycoprotein bound Hoechst 33342 from an acceptor fluorophore covalently attached to a cysteine residue in the nucleotide binding domain was determined as ~ 38 Å and the same distance for the dye LDS-751 as ~ 25 Å.^{43,44} It was also shown in kinetic experiments that LDS-751 activates the transport of Hoechst 33342 and given the large size of these ligands it is likely that they bind to P-glycoprotein in close proximity.

***In silico* prediction of cooperative binding**

So far only a few attempts have been made to predict cooperative ligand binding using computational methods. However, such methods would be valuable in drug development to minimize failure rates originating from poor pharmacokinetics and drug-drug interactions, which reduce a patient's compliance and increase the risk of medication errors. Since these problems are only revealed during clinical trials, predicting them in earlier phases of development would also reduce the number and increase the safety of *in vivo* tests. Furthermore computational methods could help predict the modifications needed for eliminating such poor pharmacokinetic parameters. Most of the molecular modeling studies dealing with cooperative binding address activation of CYP enzymes. Egnell et al. generated pharmacophore models for CYP2C9 and CYP3A4 heteroactivation^{45,46}, Shaik and co-workers performed MD and QM/MM simulations on a CYP3A4 complex^{6,7} and molecular docking has also been employed to model cooperative binding in these isoforms⁴⁷⁻⁵⁰. These models were built on compounds of limited diversity, systematic large-scale validation of computational methods predicting cooperative binding has not been published to date.

A pharmacophore model is an abstract description of steric and electronic features a ligand must possess in order to ensure optimal interactions with the receptor. These features

are typically hydrophobic and aromatic centers, hydrogen bond acceptors, hydrogen bond donors, cations and anions. Their optimal spatial arrangement and orientation is also included in the model. The pharmacophore model for activators of CYP2C9 mediated 7-methoxy-4-(trifluoromethyl)coumarin demethylation⁴⁵ was generated using 36 heteroactivators obtained from a high-throughput screen on 1504 structurally diverse compounds. The experimental parameter used for building the model was the concentration yielding 150% of control reaction rate. The pharmacophore shown in Figure 7 was generated with the Catalyst software and validated using bootstrap and leave-many-out methods. The model contained a hydrogen bond acceptor, an aromatic ring and two hydrophobic centers. It was not used to identify novel heteroactivators of the examined metabolic reaction but 65% of known inhibitors of CYP2C9 were categorized as activators by it, suggesting that activators and inhibitors of the enzyme share some common structural features. The pharmacophore model for activators of CYP3A4 mediated carbamazepine epoxidation⁴⁶ was generated using 6 heteroactivators obtained from literature sources. Model building was performed in the same way as for CYP2C9 and it contained two hydrogen bond acceptors separated by two hydrophobic centers. The pharmacophore was tested on 12 other activators for which kinetic data were available in literature and 9 were correctly identified. However, the small number of compounds used renders the relevance of the model questionable.

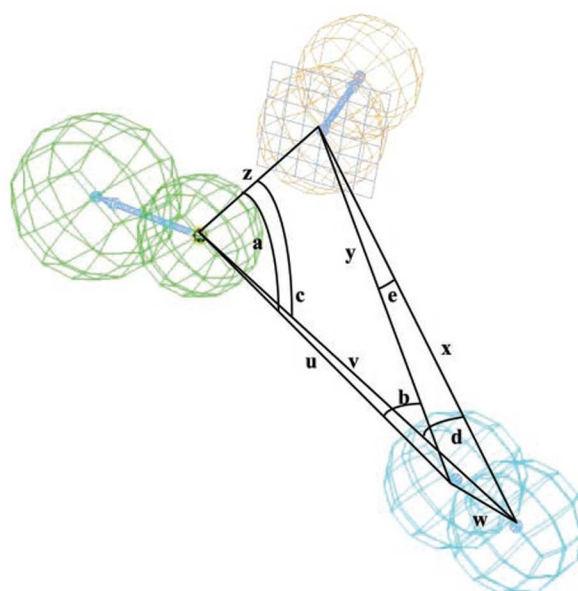


Figure 7. CYP2C9 heteroactivation pharmacophore. The green sphere represents a hydrogen bond acceptor, the orange sphere represents an aromatic ring and blue spheres represent hydrophobic features. Angles: $a = 62.2^\circ$, $b = 24.4^\circ$, $c = 67.7^\circ$, $d = 24.0^\circ$, $e = 15.9^\circ$. Distances: $u = 11.6 \text{ \AA}$, $v = 11.8 \text{ \AA}$, $w = 3.0 \text{ \AA}$, $x = 10.9 \text{ \AA}$, $y = 10.3 \text{ \AA}$, $z = 4.8 \text{ \AA}$. Figure is reproduced from ref. 45.

Molecular dynamics simulations were performed on the uncomplexed CYP3A4 and its complexes with one or two diazepam substrates by Shaik et al.⁷ The active diazepam molecule was docked in the binding site of the apo crystal structure using biological data as constraints with the PatchDock software. The effector substrate was docked without constraints and the solution with the lowest predicted binding energy was used as a starting structure for the MD run. Force field parameters for the ferryl-oxo heme and diazepam were derived from quantum mechanical computations and incorporated into the CHARMM27 force field. 6 ns trajectories were obtained for the uncomplexed and singly ligated structures while 12 ns trajectories for the ternary complex. The results indicated that the presence of the effector substrate brings about side chain reorientation particularly that of Phe213 and Phe304 but only minor long-range effects. The effector stabilizes the environment of these residues preventing them from hindering the proper orientation of the active substrate. Random snapshots were thereafter taken from the trajectories and subjected to QM/MM minimization⁶ using the B3LYP density functional and LACVP basis set with effective core potential on the iron and 6-31G basis set for other atoms in the QM region. Single point calculations were performed with the 6-31G* basis set for atoms other than iron. The QM region contained the ferryl-oxo heme together with the coordinating sulfur atom and the diazepam molecules. The results of these computations showed a decrease in sulfur and an increase in heme spin densities and a slight shortening of the Fe—S bond. This was explained by the strengthening of the N—H···S hydrogen bonds formed by Ile443 and Gly444 on the proximal side of the heme. Thus it was found that even minor long-range effects may play a role in the cooperativity between multiple substrates.

Early attempts of using molecular docking to reveal structural features of cooperative binding were made in the reports of crystal structures of CYP2C9 complexed with flurbiprofen and warfarin. In both cases the binding site seemed to be only partially occupied by the co-crystallized ligands. Therefore the prototypical flurbiprofen heteroactivator dapsone was docked to the obtained complex structure using AutoDock⁴⁷. The solution displaying the lowest predicted binding energy was selected but its validity was not confirmed experimentally. The binding mode of dapsone suggested that it might serve to limit the motion of flurbiprofen and displace water molecules in the proximity of the heme. In the case of the warfarin complex a second warfarin molecule or a fluconazole molecule were modeled into the remaining cavity of the active site⁴⁸.

Docking by Glide was performed to predict heteroactivators of CYP2C9 mediated flurbiprofen 4'-hydroxylation by Locuson et al.⁴⁹ The crystal structure of the ternary complex is not available thus the receptor used in docking was acquired from an equilibrated molecular dynamics trajectory that included both flurbiprofen and dapson. Both ligands were removed from the binding site before docking and the method was validated using 19 compounds containing 6 activators. Inhibitors either tended to have higher GlideScores than activators or their docking poses were far from the location of dapson. Based on these two observations using a GlideScore cutoff of -6.13 and a spatial filter, prediction of activation resulted in two false positives and one false negative from the test set. In the next step 77420 compounds from the ZINC database of Sigma-Aldrich chemicals were docked rigidly into the receptor containing flurbiprofen but not dapson. The 18558 compounds remaining were docked into the empty receptor structure and 5 were found exhibiting better GlideScore than dapson. The top ten scoring compounds were tested *in vitro* and the one shown in Figure 8 was found to be nearly as effective as dapson in activating flurbiprofen hydroxylation. This result, though focusing on a single metabolic reaction and docking only the effector compound to the binding site shows that docking may be used in the prediction of cooperative binding of ligands.

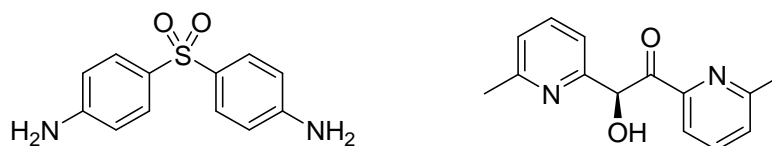


Figure 8. The structure of dapson (left) and the new CYP2C9 activator identified by Locuson et al. (right).

Finally Kapelyukh et al. used GOLD to estimate the number of 7-benzyloxyquinoline molecules able to bind in the active site of CYP3A4.⁵⁰ Using a set of 8 CYP3A4 inhibitors of differing sizes they found Hill coefficients for 7-benzyloxyquinoline debenzoylation ranging from 1.0 to 3.7 in kinetic measurements. Since n is lower than the number of binding site and substrate inhibition was still observed in the presence of bromocriptine, which produced the greatest coefficient, it was reasoned by the authors that at least 5 substrate molecules can bind in the active site. A sequential docking protocol was used in which the pose with the lowest predicted binding energy was selected in every step and merged with the protein structure. Though the crystal structure of CYP3A4 complexed with ketoconazole had already been solved, the authors used the two apo structures of the protein in the docking experiments. In

both cases five copies of the substrate were reported to provide reasonable binding energies although their orientations in these sites differed substantially and an X-ray structure verifying the relevance of either result was not obtained.

Molecular docking by Glide

Molecular docking is a computational method used to predict the preferred binding orientation and binding affinity of one molecule when it forms a stable complex with another⁵¹⁻⁵⁴. Modeled interactions are typically those between proteins and small ligand molecules, hence docking plays an important role in rational drug design. Since they are primarily used in the virtual screening of large compound libraries against one or a few receptor molecules, these methods must be very fast finding a compromise between accuracy and speed. However, more resource intensive methods have also been described for the purposes of more accurate prediction of binding affinities. Many different ways of implementation of the problem have already been developed and continuous efforts are directed towards improving these algorithms.

The protein structure used in docking is most often obtained from high resolution X-ray crystallographic experiments, sometimes from homology modeling and rarely structures determined by NMR are also used. Virtually any small molecules can be used as ligands but usually compounds from company libraries or vendor databases are screened. A significant advantage of virtual methods, however, is the ability to screen also physically unavailable molecules resulting e.g. from structure-activity relationships. The problem to be solved is actually a conformational search of the ligand structure in the reduced conformational space imposed by the receptor and the ranking of the obtained potential binding conformations. The performance of docking methods therefore depends on the searching algorithm and the scoring function utilized. Conformational search algorithms are based on systematic or stochastic torsional searches about rotatable bonds, molecular dynamics simulation or genetic algorithms to generate conformations either preliminary to the actual docking run or on-the-fly. More accurate so-called induced-fit methods also perform conformational search on the receptor, however, given the large number of degrees of freedom receptor flexibility is not routinely accounted for. Scoring functions take a candidate binding pose as input and return a likelihood value of the pose representing the true binding conformation, which not necessarily but preferably correlates with the binding free energy. Unfortunately the accuracy of the

calculation of exact binding free energy is, to date, limited even with computationally intensive methods. Common scoring functions are thus based on molecular mechanics force fields or on optimized empirical terms such as hydrophobic contacts, hydrogen bonds, frozen rotatable bonds, etc. or on a hybrid of the two. There are also knowledge-based scoring functions utilizing statistical potentials obtained from the analysis of intermolecular close contacts in 3D databases of protein-ligand complexes.

Glide (Grid-based Ligand Docking with Energetics) is a high-speed flexible docking software from Schrödinger utilizing pre-computed van der Waals and electrostatic grids of the receptors and a highly efficient series of hierarchical filters for ligand conformational selection⁶⁹⁻⁷¹. Before docking both the protein and the ligand are required to pass through a preparation procedure, which means the generation of a chemically correct three dimensional structure for both. This may involve converting from 2D to 3D, adding atoms missing in the database files, defining the correct topology and finding the possible tautomeric and protonation states at physiological pH (these steps are described in the Methods section). Schrödinger offers comprehensive structure preparation applications both for proteins (Protein Preparation Wizard) and for ligands (LigPrep) and recommends their use in combination with Glide to achieve the best results.

The first step in a docking experiment is the receptor grid generation. Van der Waals and electrostatic potentials are evaluated on the vertices of a cubic grid using the OPLS-2005 force field, which is parametrized for metals but otherwise differs little from the OPLS-2001 force field. The hard 6-12 Lennard-Jones potential is used for the calculation of van der Waals interaction energies and the Coulomb formula is used for electrostatics but with the net ionic charge on formally charged groups reduced approximately by 50%. The grid spacing far from the protein surface is 3.2 Å but it is refined progressively using cubes with edges of 1.6, 0.8 and finally 0.4 Å closest to the receptor surface. Field values at a general point in space are obtained from trilinear interpolation formulas. The origin and the spatial extension of the grid are defined by the user usually as the centroid of a ligand with known binding orientation or as the centroid of the residues forming the binding site. During this procedure the dimensions of an inner and an outer boundary box have to be specified. The potential fields are evaluated inside the outer box in which all ligand atoms must be contained, while the inner box serves to limit the possible placement of the ligand centroid. An example of the box dimensions used in this study is shown in Figure 9.

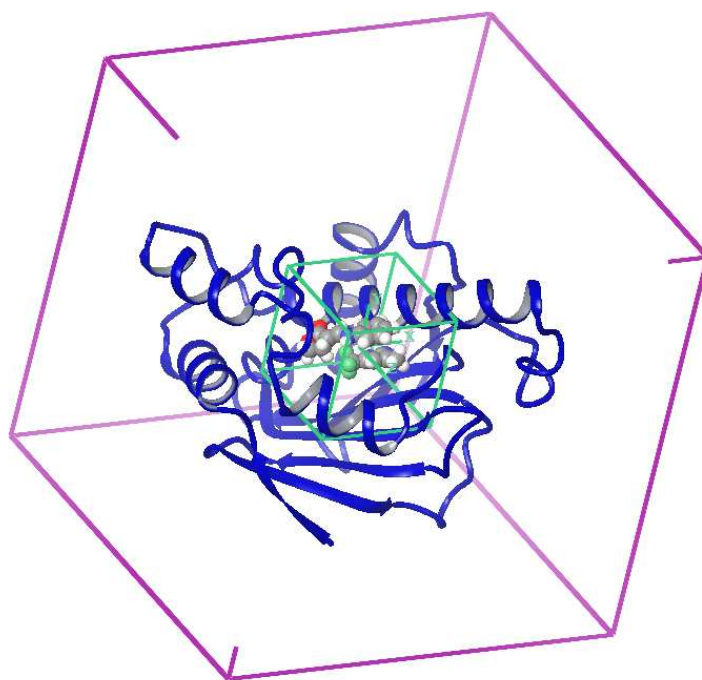


Figure 9. Inner (green) and outer (magenta) grid boundary box in Glide for the structure with PDB ID 2qfo (ribbons). The grid is centered on the centroid of the two ligands (space-filling), the edge of the inner box is 14 Å and the edge of the outer box is 36 Å.

Docking starts by an extensive conformational search of the ligand. It is first divided into a core region and a number of rotamer groups. Each rotamer group is connected to the core by a single rotatable bond and does not contain any more rotatable bonds itself thus the core is obtained by truncating each terminus of the ligand at the last rotatable bond. Core conformations are generated by sampling torsions about core rotatable bonds, different conformations of 5- and 6-membered rings and inversion of asymmetric pyramidal nitrogen centers. This results in a set of at most 662 core conformations to which rotamer end groups are later attached in all possible permutations of conformations and they are then passed to the series of hierarchical filters (see Figure 10).

The placement of the ligand to the binding site begins by choosing site-points on an equally spaced 2 Å grid in the inner box which can serve as positions for the ligand center. This is done by the comparison of the histograms obtained by binning the distances from the given site point to the protein surface and the distances from the ligand center to the ligand surface. The ligand center is defined to be the midpoint of the line connecting the two most widely separated atoms in the core region (the ligand diameter). If there is a good enough match between the histograms, the ligand center is placed at the site point and the ligand diameter is fitted in the binding site.

The ligand is then rotated about its diameter and possible hydrogen bonds and ligand-metal interactions are scored. If the score is good enough all other interaction types are scored as well using a so-called greedy scoring method. This means that the actual contribution of an atom to the total score is not the one calculated for that specific position rather the best possible score it could get by moving ± 1 Å in the x, y and z directions. This method is applied to compensate for the rough grid used for the placement of the ligand center. After this the ligand is translated as a rigid body at most ± 1 Å in the three directions and the pose with the best interaction score is passed on to the next filter. Up to this point a discretized version of ChemScore is used, while the resulting 100-400 best poses are subjected to force field minimization on the pre-computed electrostatic and van der Waals grids.

Minimization begins with a pre-minimization step on smoothed grids and ends with a full-scale annealing method on the original grids sampling translations, rotations and torsional motions of the ligand molecule. Finally torsions are further sampled by a Monte Carlo procedure. The resulting poses are ranked using the Emodel scoring function and the predefined number of top poses is saved. The saved poses are re-scored and also re-ranked using the GlideScore scoring function. Thus Emodel is used for pose selection and GlideScore is used for predicting the binding affinity of the selected poses. Both scoring functions are developed by Schrödinger, they are available exclusively in Glide and no exact details on them were published so far. GlideScore is known to contain van der Waals and Coulomb energy terms, rewards for hydrophobic interactions and for polar but non-hydrogen-bonding groups in a hydrophobic environment, a hydrogen bonding term handling neutral-neutral, neutral-charged and charged-charged hydrogen bonds differently, a metal binding term and penalties for freezing rotatable bonds and inadequate solvation of functional groups not involved in close contacts. Solvation in Glide is modeled by placing explicit water molecules in the vicinity of the docked ligand. Emodel contains these same terms plus contribution from the ligand-receptor molecular mechanics interaction energy and ligand strain is also incorporated in it.

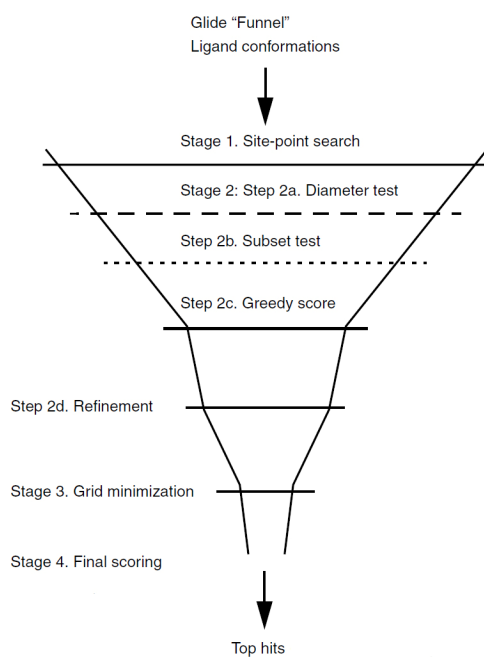


Figure 10. Visual representation of the hierarchical filters applied by Glide. Figure is reproduced from the Glide User Manual.

Glide provides an extra precision (XP) docking mode for the minimization of the number of false positive hits and higher correlation between experimental and predicted binding affinities. The XP procedure performs a refinement on the poses obtained from a single precision (SP) docking run with less forgiving scoring methods. An anchor fragment of the docked ligand, typically one or a few rings, is taken from the best-scoring SP poses and the rest of the molecule is grown bond by bond from this anchor. The generated large ensemble of poses is subjected to a more comprehensive scoring than in the SP mode with improved terms in the GlideScore scoring function. Instead of lipophilic pair terms multi-center enclosure terms are calculated for apolar groups. The scoring of hydrogen bonds, the detection of cation- π and π - π stacking interactions and the modeling of solvation are also improved.

Comparison to other docking tools

There is a variety of docking software available and most of them differ greatly in the details of their implementation⁵¹⁻⁵⁴. One aspect to consider is how they treat the ligand during docking. While Glide removes only terminal rotamer groups from the ligands, DOCK, FlexX and HammerHead use an incremental build-up strategy. For example FlexX severs all noncyclic bonds of the ligands and all of the resulting base fragments are used as starting

points for the docking procedure. The correct rotameric state of each group added is chosen by evaluating a specific scoring function for the fragment. On the other hand individual ligand conformations are treated in their entirety by e.g. GOLD, ICM-Dock, FRED, Surflex and AutoDock, a free open source docking program.

Softwares also differ in their implementation of the search strategy. Glide along with those that use the incremental build-up approach aims at an exhaustive enumeration of ligand conformations. FRED also uses a pre-generated ligand conformer library of at most 200 members and docks every conformer using soft Gaussian functions to represent the ligand surface. This error-tolerant scoring compensates for the low number of generated conformers and a more detailed follow-up scoring is employed. Surflex uses an interesting search algorithm. First it generates an ideal ligand for the receptor, a so-called protomol from N-H, C=O and C atom fragments, then aligns every conformation of the ligand to it and finds the ones with maximal molecular similarity, which are further refined. The remaining programs mentioned above employ stochastic search algorithms: ICM-Dock uses pseudo-Brownian sampling, GOLD uses a genetic algorithm while AutoDock provides a Lamarckian and a traditional genetic algorithm and Monte Carlo simulated annealing as well (best performance is reported for the Lamarckian algorithm). The genetic algorithm of GOLD assigns chromosomes to each receptor-ligand complex that contain information about the ligand conformation and position, rotatable hydroxyl and amino groups of serine, threonine, tyrosine and lysine residues in the binding site as well as hydrogen bonds and lipophilic interactions. Genetic operators are applied to the chromosomes in each step and the fitness is computed using a scoring function after decoding the chromosome to the 3D ligand pose. It is worth noting that GOLD and FlexX attempt to account for water molecules not displaced by the ligand. They evaluate possible locations for water molecules in the binding site prior to docking and either retain or remove these waters during the docking run. Minor improvements in performance have been reported for both programs upon the implementation of water treatment.

Given the considerable number of docking applications to choose from, one needs a means of comparing their accuracy in binding mode prediction and performance in virtual screening. The first question is most often addressed by comparing the root mean square deviations (RMSDs) between corresponding atomic positions of the experimental and the predicted binding modes. A docking run is usually deemed successful if the top scoring pose has an RMSD lower than 2 Å. This definition mirrors typical screening applications, which

save only a single pose and it is thus comparable across different docking programs. The case when the top scoring poses have higher RMSDs but other saved poses have RMSDs $< 2 \text{ \AA}$ is termed scoring failure, since a more accurate scoring function may improve overall performance. However, when none of the generated poses have RMSD $< 2 \text{ \AA}$, then improvement cannot be achieved by rescoring. This case is termed sampling failure.

Performance of docking softwares in virtual screening situations is usually evaluated carrying out enrichment studies. In these studies a set of ligands containing both known active and decoy compounds is docked to a receptor target and the ability of the program to separate the two groups is assessed. There are several metrics used for this aim: enrichment factors or curves, receiver operating characteristic (ROC) values or curves and the area under the ROC curve (AUC). The enrichment factor is the fraction of recovered actives in the first $n\%$ of the ranked list of compounds, usually the top 1-10%. An enrichment curve is the plot of the enrichment factor at $n\%$ against n . The ROC value is the fraction of recovered actives after $n\%$ of the decoys are recovered and the ROC curve is the plot of the ROC value at $n\%$ against n . The advantage of the latter over enrichment curves is that they are independent of the proportion of actives in the test set. In the compilation of the test set it is recommended that decoys follow the same distribution of formal charge, molecular weight, logP and ligand surface area as actives because scores may correlate with these parameters. The DUD (Directory of Useful Decoys) set is a publicly available data set used frequently in enrichment studies. It consists of 40 protein targets each with a set of molecules known to be active against the protein target and 36 decoys for each active ligand.

One of the most extensive comparisons of docking programs is that by Warren et al. from GlaxoSmithKline⁵⁵. In this study 10 docking tools (Dock4, DockIt, FlexX, Flo, FRED, Glide, GOLD, LigFit, MOE and MVP) were compared in setups resembling the ones frequently used in pharmaceutical research. The aim of the authors was to standardize the evaluation of the softwares to the highest extent and reduce the bias originating from different extents of expertise in the usage of the programs. It thus needs to be noted that the protein and ligand preparation steps were performed using different methods and force fields that are recommended by Schrödinger in connection with using Glide. The test set included 8 protein targets of 7 protein types with a total of 1303 ligands being the members of 2 to 5 congeneric series per protein with affinities spanning at least 4 orders of magnitude. The affinities were required to have been measured in a consistent assay format. Also 136 crystal structures of these protein-ligand complexes were available. The comparison was performed assessing

three aspects of performance: binding mode prediction using RMSDs, virtual screening for lead identification using enrichment curves and rank-ordering by affinity for lead optimization using the correlation coefficients between measured and predicted binding affinities.

The most important message of this publication is that no single program performed well across all protein targets but there was at least one program able to predict the correct binding modes of 40% of the ligands for each target. Only GOLD and Glide provided poses with $\text{RMSD} < 2 \text{ \AA}$ for some ligands of each target, other softwares failed to dock all ligands of at least one target. GOLD was able to reproduce 70% of the experimental binding modes while Glide reproduced only 45% of the examined complex structures. The ratios of well-docked top ranking poses are 43% and 34% for these programs, respectively. In virtual screening setups MVP provided the best overall performance with 57% average enrichment in the top 10% of the docking score ordered ligand lists, FlexX following with 33% and Glide with 29%. There were 4 targets where Glide exhibited high enrichment rates, while for the other 4 targets (2 of them metalloenzymes) these were comparable to the random distribution of actives in the ligand set. Finally, no strong correlation between measured and predicted binding affinities was observed for any software or target protein. Even though in this study Glide did not prove to be outstanding, it provided reasonable results both in pose reproduction and virtual screening. However, the reason for this may have been the not ideal preparation methods and the small number of protein targets.

Another study by Kontoyianni et al. evaluated the ability of 5 docking tools (DOCK, FlexX, Glide, GOLD and LigandFit) to reproduce experimental binding modes against a set of 69 protein-ligand complexes from the PDB belonging to 14 protein families⁵⁶. In this work all docking solutions were inspected visually and evaluated on the basis of the RMSDs of the docked ligands. The solutions were classified in a subjective manner as close (capturing important interactions), active site (mainly right but a few ligand groups misoriented) or inaccurate. Here again observed success rates were highest for GOLD and Glide. 68% and 57% of the docked poses with the lowest RMSDs among the 60 saved poses were respectively classified as close ones but Glide provided significantly lower ranks for these best poses. Glide ranked the pose with the lowest RMSD top in 25% while GOLD in 14% of the cases. It was also observed that GOLD failed mostly for hydrophobic binding sites while Glide was less discriminatory in regard to the nature of the polarity of the sites. A study by Cummings et al. using a somewhat more restricted test set of 49 known ligands of 5 protein targets comparing 4 docking tools (DOCK, DockVision, Glide and GOLD) in virtual screening

setups also found that Glide gave the most consistent level of success, though GOLD achieved greater success with some targets⁵⁷.

A more recent work by Cross et al. compared 6 docking programs (DOCK, FlexX, Glide, ICM-Dock, PhDOCK and Surflex) including a newer version of Glide (v4.5) both assessing binding mode prediction using RMSDs and virtual screening using ROC curves⁵⁸. The test set for the former comprised 68 diverse, high-resolution X-ray complexes representing recent pharmaceutical interests while for the latter the DUD set was used. The bias originating from different extents of expertise with the softwares was reduced by using default settings everywhere. ICM-Dock and Glide were found to provide the lowest mean and median RMSDs and also the lowest standard deviations of the RMSD values in binding mode prediction. They also showed very similar RMSD distributions (see Figure 11) with about 80% of the experimental binding modes reproduced with $\text{RMSD} < 2 \text{ \AA}$ regardless of ranking and 70% reproduced as top ranked poses. These figures also indicated a major improvement over earlier versions of the programs. In virtual screening setups the high throughput version of Glide was used, which uses a smaller extent of conformational sampling but even so Glide yielded the highest mean AUC value 0.72 for all 40 protein targets. The second highest value 0.66 was obtained for Surflex. Also the ROC values at 0.5, 1, 2, 5 and 10% of the recovered decoys were highest for Glide followed by DOCK and ICM-Dock (see Figure 11 for an example ROC curve).

An extension of this work was later performed by McGann including FRED in the comparison of the softwares and employing a rigorous statistical analysis of the results⁵⁹. It was found that Glide outperforms ICM-Dock with a probability of only 52% while other programs with 60-70% in a single structure reproduction docking experiment. However, it will outperform ICM-Dock with a probability of 65% while other programs with 90-100% on average in structure reproduction. This again indicates a strong dependence of software performance on the particular protein target. Findings were similar for virtual screening with Glide outperforming other programs with a probability of 60-80% in a single screen while with 80-100% on average. A recent study on 190 protein-fragment complexes³⁹ revealed that in addition to docking druglike compounds Glide is adequate for fragment docking even in cross-docking setups. Based on these reports it can be stated with confidence that Glide is one of the most reliable choices in docking experiments.

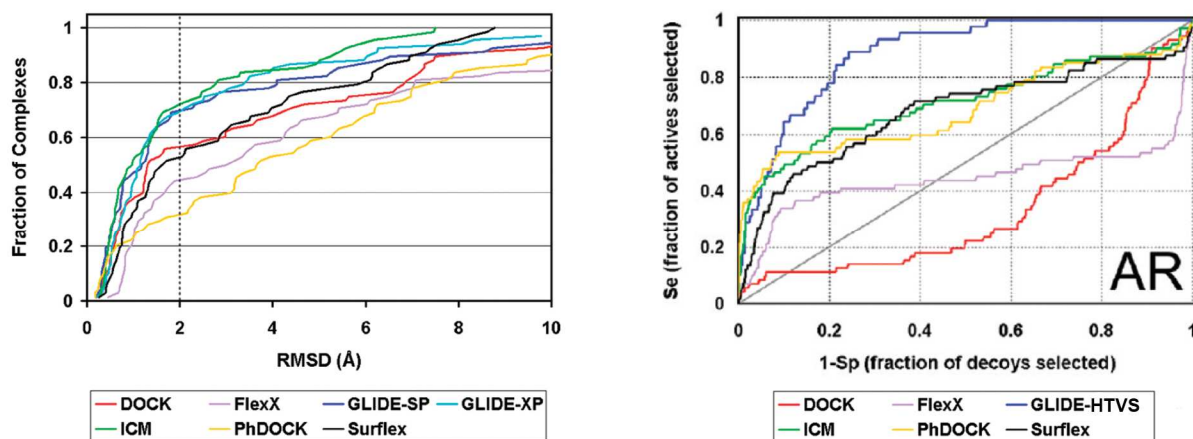


Figure 11. Cumulative RMSD distribution plot of top poses in cognate ligand docking from the study by Cross et al. (left) and a representative ROC curve for the androgen receptor target in the DUD data set from the same study (right). The vertical line on the left indicates the RMSD cutoff for well-docked poses, the diagonal line on the right indicates random selection of ligands. Figures are reproduced from ref. 58.

Experimental section

Methods

Assembly of data set

X-ray protein-ligand complex crystal structures used in this study were selected from the PDB. Initial filters included a resolution of at least 2.5 Å, protein-only structures, thus excluding DNA and RNA binding proteins and no appearance of words associated with photosynthesis or the words MEMBRANE and IMMUNE in the HEADER entry of the pdb files. The structures were required to have ligands not present in a pre-defined list of excluded ligands. This list contained the hetID codes of water, deuterated water, common cations and anions, common solvents and crystallization agents including PEGs, buffer constituents, lipids, disulfide bond reducing agents etc., known coenzymes and prosthetic groups, common carbohydrates and carbohydrate-amines (e.g. NAG), modified residues present in the respective structure, and the unknown species UNL and UNX. The number of non-excluded ligands was then determined, those covalently linked to the protein were discarded and pairwise minimal interatomic distances between the remaining ligands were calculated. A graph with vertices as these ligands having edges between ligands not farther away from each

other than 6.0 Å was defined. If its maximal connected subgraph had at least two and at most six vertices and there were no cations, anions, coenzymes and prosthetic groups except for heme in the 6.0 Å neighborhood of this ligand cluster, the structure was saved. The saved structures were finally visually inspected to eliminate cases where the structure contained incorrectly defined connectivity or atoms not parametrized in the OPLS-2005 force field.

This filtering of the PDB resulted in 115 structures as of 1 November 2010. These structures thus have good resolution and contain a cluster of at least two and at most six ligands in close proximity to each other (see the distribution of ligand numbers in Table 2). They are also suitable for docking experiments since they do not contain structural features not handled by the force field used by Glide. Two of these protein-ligand complexes (1e7c and 3g35) had two distinct, non-symmetry equivalent sites where multiple ligands were present. The docking procedure in these cases was performed for both binding sites and the total number of experiments thus increased to 117. PDB accession codes and chain identifiers of the structures are listed in the appendix.

site property		count
all sites		117
contains 2 ligands	same ligand	83
	different ligands	11
contains 3 ligands		14
contains 4 ligands		7
contains 5 ligands		1
contains 6 ligands		1
contains only Lipinski compliant ligands		94

Table 2. Characteristics of the cooperative docking data set.

Structure preparation

The most completely modeled biological assembly in the unit cell was retained from the crystal structures. If the biological assembly contained crystal mates, only chains in the vicinity of the docked ligands were added. In cases where there were more identical chains in the unit cell, the first chain containing the multiply ligated site was selected. Further phases of the work were automated using the Schrödinger Python API available in Schrödinger Suite 2010 (version 3.8). The structures were prepared for docking with the Protein Preparation Wizard⁶⁰ using the following default steps: assigning bond orders, adding hydrogens, treating metals, creating disulfide bonds, converting selenomethionines, deleting far waters, assigning

the H-bond network with water sampling and finally minimizing the structure up to 0.3 Å RMSD with the OPLS-2005 force field. All waters and docked ligands were then deleted from the structures before grid generation.

The docked ligands were prepared by converting them first to 2D structures with the ChemAxon molconvert plugin⁶¹ and converting them back to 3D with the Schrödinger LigPrep 2.4 application⁶² retaining the configuration of chiral centers. This was done to eliminate the conformational bias of using experimental binding modes. Tautomers were generated and Epik 2.1⁶³⁻⁶⁵ was used to generate protonation states at pH 7±2. When the protein was crystallized outside of this range, it was verified that LigPrep found no additional protonation states on the pH of crystallization. Common physico-chemical properties of the ligands were calculated with the ChemAxon cxcalc plugin⁶⁶ and their druglikeness was assessed by applying Lipinski's rule (MW ≤ 500 Da, logP ≤ 5.0, hydrogen bond acceptor count ≤ 10, hydrogen bond donor count ≤ 5).

Protein binding sites were characterized by using the Schrödinger SiteMap 2.4 application⁶⁷ in single binding site region evaluation mode with a 6 Å buffer around the docked ligand cluster (default parameter). From these calculations the estimated site volume, exposure and enclosure values were inspected as we hypothesized they may have direct effect on the quality of docking experiments. The exposure parameter is the ratio of the number of so-called extension site points to the sum of original and extension site point numbers. A shallow surface site allows the placement of more extension site points than a closed one, thus lower values of this parameter mean a more buried site and the average for a tight-binding site is given to be 0.49. Enclosure is defined by the number of radial rays drawn from the site points intersecting the receptor surface within 10 Å to the number of all radial rays drawn from the site points. Here a higher value means a more buried site and the average for a tight-binding site is given to be 0.78. There were four structures where SiteMap did not find a site but in order to quantify this data these complexes were assigned a value of 1.0 for exposure and 0.5 for enclosure, the values for a hypothetical site with no site points on a planar protein surface. See Figure 12 for distributions of crystallographic and calculated properties of sites and ligands.

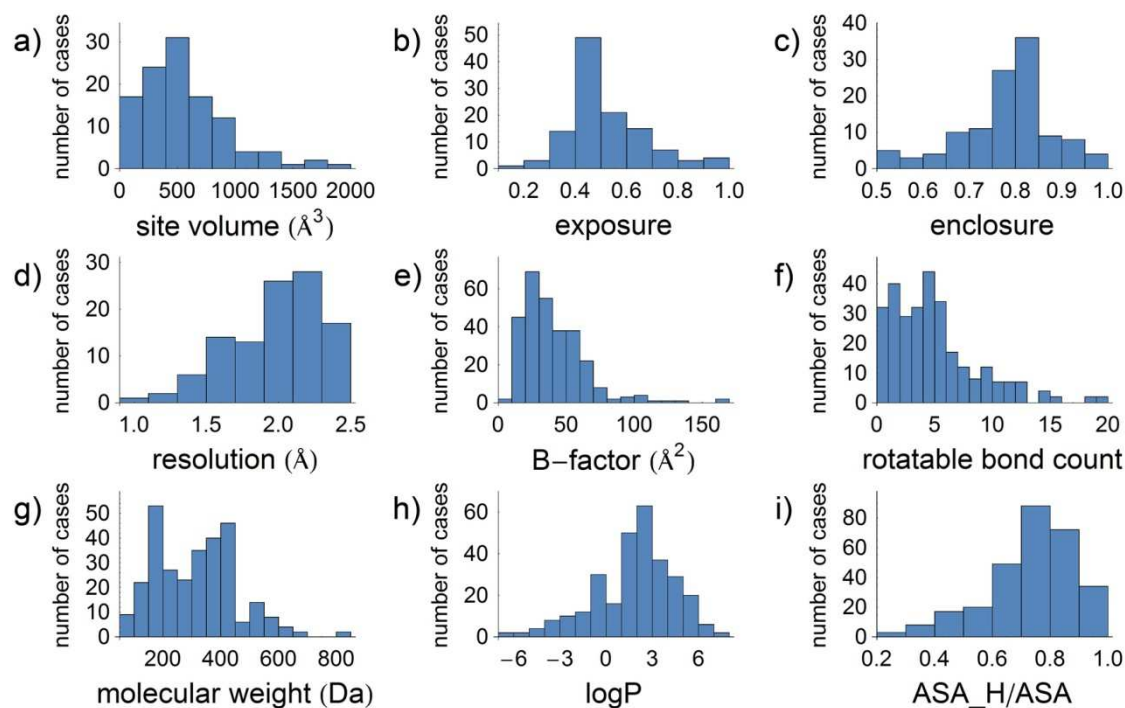


Figure 12. Distribution histograms of structure (a-d) and ligand (e-i) properties calculated with SiteMap (a-c), obtained from crystallographic data (d-e) and calculated with cxcalc (f-i).

Docking protocols

Docking was performed by Schrödinger Glide 5.6⁶⁸⁻⁷¹ using both Single Precision (SP) and Extra Precision (XP) algorithms. A docking run for one structure consisted of at most as many consecutive grid generation and docking steps as the number of ligands in the docked ligand cluster. The maximum available grid size (36 x 36 x 36 Å³ outer and 14 x 14 x 14 Å³ inner box) was used and the grid was always centered on the centroid of the heavy atoms of all ligands in the cluster, thus the grid was positioned the same way in each step of a run. The first grid was generated for the receptor not containing any of the docked ligands. In the docking steps each protonation state and tautomer of the ligands were docked with three different set of settings. As a default Glide scales down van der Waals radii of nonpolar ligand atoms with partial charge less than 0.15 by a factor of 0.8. Our three docking protocols included SP with such scaling applied, XP with scaling and SP with no scaling of ligand vdW radii (hereafter referred to as hard docking). The number of poses included in post-docking minimization and saved was always set to 30 while for other parameters default values were used. RMSDs between docked and experimental ligand conformations were calculated using only heavy atom positions.

In the case of multiple copies of the same ligand from the first docking step the pose carried on to the further steps was selected as follows: if all RMSDs between all docked poses and all experimental binding conformations were greater than 2.0 Å then the whole run was terminated as it means that a satisfactory pose cannot be found for any of the remaining ligands. For the sake of being able to examine the RMSD distribution of the docked poses, this restriction was removed for the first SP scaled procedure. Then if the first docked pose (default ordering of the poses by GlideScore value was used) of any protonation state or tautomer of the ligand had an RMSD less than 2.0 Å to any of the experimental ligand conformations, that pose was selected. If there were more such, the one with the least RMSD was selected. If there were none then the second poses were inspected in the same way then the third poses and if these still not had RMSDs less than 2.0 Å then the pose with the least RMSD of all remaining poses was selected. After selecting the pose to go on with, this ligand conformation was merged with the protein structure and a new grid was generated as described earlier. Then the second copy of the ligand was docked in the same way and so on until the ligand cluster has been exhausted. In this way the order of docking the ligands of the cluster did not need to be defined as is the case when docking ligands with unknown binding conformations. However, when different ligands are present at the site, every permutation has to be evaluated because in such cases their binding order may not be obvious. In these cases RMSDs have to be calculated only for the respective experimental conformation. As only structures containing two different ligands were found, this meant two possible docking orders, which were otherwise the same as in the case of similar ligands.

Since GlideScore is primarily used for the comparison of binding efficiencies of different ligands while the Emodel value ranks the poses within a single docking experiment⁴⁹ the results were re-evaluated using Emodel based ordering of poses. Furthermore a third Glide Energy based ordering was tested as well. First we performed the re-evaluation by rescoring the saved poses with Emodel in a GlideScore ordered protocol but next we repeated all docking runs using the Emodel based ordering in pose selection as well. Qualitative differences between the two pose selection methods were encountered in only a few cases. In the SP protocol there was one site containing four ligands (3em0) where three could be docked with RMSDs lower than 2.0 Å when poses were selected by GlideScore but only two were well-docked when selecting the poses by Emodel. There was another site with three ligands (1n8v) exhibiting the reverse case and there was one site containing two ligands (2xuc) where well-docked poses could be found for only one by GlideScore while Emodel

afforded two well-docked ligands. All other docking runs provided the same numbers of well-docked ligands. In the XP protocol there were two cases (1e7c, 2zeb) when the GlideScore based method afforded only one well-docked ligand while using Emodel provided two. There was one structure (1gnw) exhibiting the reverse case. In the SP hard docking protocol there were four cases with qualitative difference. One of them (2uxi) where two and one ligand could be docked using GlideScore and Emodel ranking, respectively, and one case (2whf) where the reverse situation was found. Finally, one case (2a3b) where one and three ligands could be docked and one case (3p2r) where three and two ligands could be docked, respectively. Qualitative differences between pose ranks in the re-run and re-evaluated Emodel based method using the three categories top, top three and any pose were found for 8 docking steps (out of 291) in the SP, 2 docking steps in the XP and 6 docking steps in the SP hard protocol. Since these findings mean only marginal differences in statistics only the re-evaluated results of the GlideScore ordered protocol are reported hereafter except for case studies. The data collected from the docking runs are thus the RMSDs of the selected poses and their ranks with the three different ordering methods.

Results

Overall performance in binding mode reproduction

Our data set of 117 receptor sites contained a total of 269 ligands to be docked, which means an average of 2.3 ligands per binding site. The reverse order cases with different ligands at the sites increased the number of required docking steps to 291 in each of the three protocols and orderings of poses. A full list of RMSD values calculated between the docked and the experimental ligand binding conformations was only obtained for the SP GlideScore ordered protocol, in other procedures values greater than 2.0 Å were truncated. The average RMSD for the selected poses in all the 291 docking steps was 2.53 Å, which is greater than the commonly used 2.0 Å cutoff for well-docked poses. A pose within 2.0 Å among the 30 poses saved could be identified in only 57% percent of the cases but these results contain all values of ligands docked in each steps of a docking run. The lowest RMSD was 0.20 Å while the highest was 11.86 Å. When these results were decomposed according to docking order an average RMSD of 1.52 Å (min: 0.20 Å, max: 6.88 Å) and success rate of 74% was obtained for ligands docked first. An average RMSD of 2.51 Å (min: 0.20 Å, max: 8.73 Å) and success rate of 56% was obtained for ligands docked second. In 8 out of 23 cases could a third ligand

be docked regardless of the results of the previous steps with lower RMSD than 2.0 Å. More than three ligands could never be docked within this limit. Figure 13 shows the distribution of these RMSD values. It can be seen that for the first ligands the distribution falls off more rapidly than for the second ones, while for the third ligands it is almost uniform.

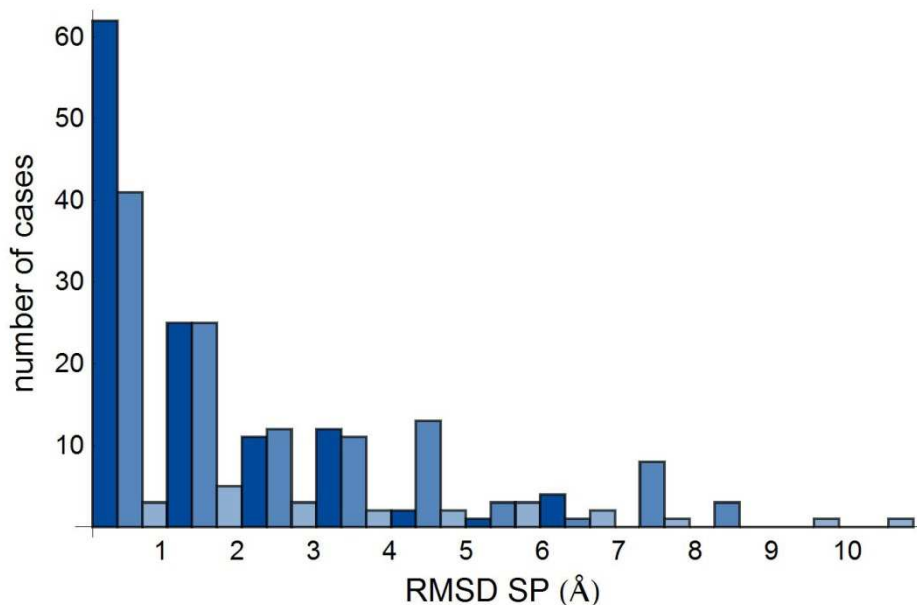


Figure 13. RMSD distributions of ligands docked first (dark blue), second (mid blue) and third (light blue).

The effect of ligand number on docking performance

The most important performance measure in our study was not the overall performance of Glide in the individual docking steps rather the number and quality of consecutive docking steps where a well-docked ligand pose could be found. This metrics allows the estimation of the probability that all sequentially docked ligand poses represent true binding conformations. Usually many ligands can be docked into a large enough grid but the relevance of docking more than one ligand was so far unknown. By comparing these docking runs to existing protein-ligand complexes one can assess the likelihood for success in a sequential docking procedure when experimental information is not available. To address this question we looked at the number of consecutive docking steps where a pose with RMSD < 2.0 Å could be found at all among the 30 saved poses and its dependence on the number of ligands present at the binding site.

This analysis showed differences between the SP, XP and SP hard docking protocols but no substantial differences between GlideScore based and Emodel based ranking schemes (see Table 3 for comparison). Out of the 94 sites with two bound ligands there were 52 cases in the SP GlideScore ordered protocol where both ligands could be docked, 20 cases where only one could be docked and 22 cases where not even the first step resulted in an acceptable pose. Out of the 14 sites with three bound ligands in 4 cases could all three ligands be docked, in 4 cases two could be docked, in 2 cases only one could be docked and in 4 cases not even one ligand could be docked. Four ligands could never be docked to the 7 receptors containing this number of ligands in the experimentally determined structures and in 2, 1, 1 and 3 cases could three, two, one and no ligands be docked, respectively. To the sole structure with five ligands only two of them could be docked and no acceptable poses were found when docking to the site containing six ligands. These figures add up to an expectation value of 1.34 for the number of successful docking steps. Based on this and the finding that in only 6 out of 23 cases could a third ligand be docked with a pose having an RMSD $< 2.0 \text{ \AA}$ it can be concluded that the successive docking of more than two ligands is highly unlikely to give reliable results. Even with two ligands there is only a chance of 55% to recover both of their experimental binding conformations.

The XP GlideScore ordered protocol provided lower numbers of well-docked ligand poses than the SP protocol. RMSDs are usually similar or lower than those obtained from the SP protocol but when the rank order of the selected pose is higher (usually if greater than 6th), XP tends not to find that pose at all. There were only 8 docking steps (out of 291) where XP found a pose within 2.0 \AA while SP did not and 54 instances of the reverse situation. Thus it seems that XP only sorts out poses with higher scores and is not able to score them better than SP in the scenario of multiple ligands occupying a receptor site. The expectation value for the number of successful docking steps with XP was 0.97 and the chance to recover at least two experimental binding conformations was 35%. The SP hard GlideScore ordered protocol provided similar RMSDs to the default SP algorithm. There were 11 steps where the SP hard protocol found a pose within 2.0 \AA while SP did not and 10 instances of the reverse situation. The expectation value for the number of successful docking steps was 1.37 and the chance to recover at least two experimental binding conformations was 57%, slightly better than with SP.

number of ligands in site	number of sites	number of docking runs with n successful consecutive docking steps											
		SP					XP					SP hard	
		0	1	2	3	n=	0	1	2	3	n=	0	1
2 ligands	94	22	20	52	-	36	24	34	-	24	18	52	-
3 ligands	14	4	2	4	4	6	4	4	0	3	1	5	5
4 ligands	7	3	1	1	2	1	3	2	1	2	1	3	1
5 ligands	1	0	0	1	0	0	1	0	0	0	0	1	0
6 ligands	1	1	0	0	0	1	0	0	0	1	0	0	0
total	117	30	23	58	6	44	32	40	1	30	20	61	6

Table 3. Number of well-docked (RMSD < 2.0 Å) ligands per binding site using different protocols depending on the number of ligands present at the site.

The effect of docking order on docking performance

When docking multiple different ligands, it is a question in which order to dock them. In this study both permutations were evaluated. However, there were only 11 structures in our data set containing two unique compounds, which does not give a firm basis for drawing far-reaching conclusions regarding this issue. Out of these 11 cases there were 3 where neither docking order provided any well-docked poses for either of the ligands. In 2 cases one ligand could be docked with an RMSD within 2.0 Å in one of the permutations, while none in the other. 3 docking runs provided two well-docked ligands in one order and none in the other. Finally in 3 cases both ligands could be docked in both directions but one of them was always clearly superior to the other based on RMSDs and rank orders of the selected poses. GlideScore and Emodel based ranking gave similar results with the default SP protocol. Visual inspection suggested that the better performing docking order was that docking the inner, more buried ligand first and the ligand more or less exposed to solvent second as expected. It was also found that if comparing the two top ranked poses of the ligand with higher average GlideScore (the worse binder) the one with the lower GlideScore value came from the superior docking order in 8 out of 11 cases. This observation suggests that the docking order scoring the worse binder better should be used when docking non-native ligands but more data would be needed to investigate its validity.

Docking performance on the druglike subset

Next it was examined whether the described method of sequential docking presents improved performance in different subsets of the initial data set obtained by applying several filters. It was expected that the docking of druglike ligands would be more efficient since the GlideScore scoring function was optimized against a set of known binders of pharmaceutical targets and decoys with drug- and lead-like structural feature distributions^{49,50}. In this work ligands were classified as druglike if they did not violate any of Lipinski's rules. It was also expected that docking to shallow and open binding sites would be more challenging since the ligand cannot exploit as many binding interactions as in a closed binding site and the scoring of surface bound conformations is thus more difficult. The exposure and enclosure values calculated by SiteMap were used for the classification of binding sites to open and closed ones. Possible dependence of docking accuracy on resolution, relative B-factors (the ligand's mean B-factor divided by the whole structure's mean B-factor) and the ligands' physico-chemical parameters were also examined. These, however, showed only weak trends: average and lowest RMSDs increased slightly with increasing relative B-factor and number of rotatable bonds of the ligands. There were no ligands docked with $\text{RMSD} < 1.0 \text{ \AA}$ containing more than 9 rotatable bonds and none with $\text{RMSD} < 2.0 \text{ \AA}$ containing more than 12. No correlation between resolution and docking accuracy was found in this particular set composed only of good quality structures.

The selection of structures complexed with druglike ligands only resulted in a 94 member subset of the original 117 sites. In the default SP protocol combined with GlideScore ranking the fraction of cases where a well-docked ligand pose ($\text{RMSD} < 2.0 \text{ \AA}$) could be found in at least two consecutive docking steps increased from 55% for all structures to 62% for this subset (for comparison of all data in this section see Figure 15). In addition, the cases where the selected pose was among the three top ranking poses and also when the selected pose was the top ranking pose itself were enumerated. This was done because if ligands with unknown experimental binding conformations are docked it is most desirable that the top ranking pose represent a true binding mode. The fraction of cases with the selected pose being among the top three poses increased only slightly from 35% to 38% in the druglike subset and the fraction with the selected pose being the top ranking pose from 25% to 27%. With the re-evaluation of the results using Emodel based ranking of poses in every docking step the fractions of structures with any, top three and top ranking well-docked poses increased respectively from 55%, 38% and 29% for the whole data set to 62%, 43% and 32% for the

druglike subset. With re-evaluation using Glide Energy based ranking the initial 55%, 34% and 29% increased to 62%, 37% and 32% when applying this filter. From these figures it can be concluded that both Emodel and Glide Energy performed slightly better in ranking the poses within one docking step in the SP protocol than did GlideScore as they provided a higher ratio of top ranked well-docked binding conformations. The druglike subset exhibited only moderate improvement over the whole data set.

The XP and SP hard protocols presented similar behavior for the druglike subset but they gave different results earlier for the whole data set. In the XP GlideScore ordered protocol ratios of cases with two successive docking steps with any, top three or top ranking well-docked poses were 35%, 26% and 22% respectively, which increased to 40%, 30% and 26% in the druglike subset. The smaller separation between these percentages than in the SP protocol indicates that when XP finds the true binding conformation at all, it is able to rank it top with a higher probability. Thus the fraction of structures with two top ranking well-docked poses is only moderately lower for XP than for SP. In regard of the selection of the scoring function for pose ranking there were even smaller differences between GlideScore, Emodel and Glide Energy than in the SP protocol. In the SP hard GlideScore ordered protocol ratios of cases with two successive docking steps with any, top three or top ranking well-docked poses were 57%, 39% and 31% respectively, which increased to 64%, 44% and 33% in the druglike subset. These values are somewhat higher than that for the default SP protocol utilizing scaling of nonpolar ligand atom van der Waals radii but the separation between the percentages are very similar for the two protocols since the scoring function is the same in both cases. Emodel based ranking in this protocol provides slightly better ratios of well-docked top ranked poses, while ranking by Glide Energy gives similar results as GlideScore based ranking.

Docking performance on the closed site subset

In evaluating the closedness of binding sites first the average values of the exposure and enclosure parameters for a tight-binding site given in the SiteMap user manual were used to categorize them. Partitioning of the binding sites by their exposure values at a cutoff of 0.49 classifies 56 of them as open and 61 as closed. Out of the 61 closed sites there were 41 (67%) where a docking pose with RMSD lower than 2.0 Å could be found in at least two consecutive docking steps in the SP protocol with GlideScore ranking. Out of the 56 open

ones there were 33 (59%) where a well-docked pose was not found in two consecutive steps. Partitioning by enclosure values at a cutoff of 0.78 classifies 46 of the binding sites as open and 71 as closed. Here out of the 71 closed sites there were 49 (69%) where a docking pose within 2.0 Å to the experimental binding conformation was found in at least two successive steps. Out of the 46 open ones there were 31 (67%) where a well-docked pose could not be found in at least two consecutive steps.

The higher ratios of successful docking runs among closed sites and unsuccessful docking runs among open sites and the broader distribution of the enclosure parameter (see Figure 12) suggested that enclosure is superior to exposure in distinguishing between open and closed sites. This observation prompted us to find an optimal cutoff value of the enclosure parameter for the classification of sites. It was conceived that a good partitioning would sort as many sites as possible where at least two successive docking steps resulted in well-docked poses into one group and as many sites as possible where this was not the case into the other. Thus for enclosure the following threshold parameter was defined, whose maximum value corresponds to the optimal enclosure cutoff to divide sites into an open and a closed subset:

$$\frac{\text{no. of unsuccessful runs in open sites}}{\text{no. of open sites}} + \frac{\text{no. of successful runs in closed sites}}{\text{no. of closed sites}}$$

The value of this formula is 1 for a fully random distribution of successful and unsuccessful docking runs over the range of sites sorted by their enclosure parameter and 2 for the perfect partitioning when docking runs are successful for all closed sites and unsuccessful for all open sites. Meaningfulness of the above formula requires that both open and closed subsets have sufficient populations for the calculation of ratios, which in this study was set as at least 15 elements per group. Two greater local maxima inside these limits were found: one occurs when dividing between the sites possessing enclosure values of 0.713 and 0.725 while the other occurs if dividing between the sites with enclosure 0.811 and 0.814 (see Figure 14). Since the latter would have provided only 46 closed sites instead the cutoff of 0.72 between the former values was used in the further investigations, which classified 91 sites as closed. Out of these there were 59 (65%) where a docking pose with RMSD lower than 2.0 Å could be found in at least two consecutive docking steps. Out of the 26 open sites there were 21 (81%) where a well-docked pose was not found in two successive steps.

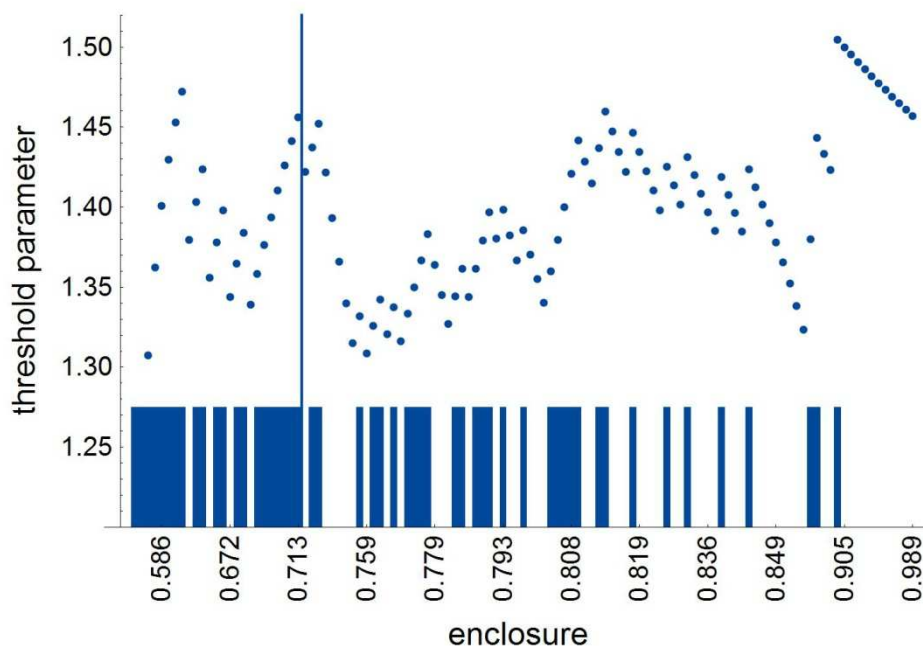


Figure 14. The threshold parameter with different enclosure cutoffs for partitioning sites into an open and a closed subset (points). Full vertical bars correspond to unsuccessful docking runs, empty bars correspond to successful runs and the vertical line corresponds to an enclosure value of 0.72 used in this study for the partitioning. Note that the enclosure axis is not linear but represents only the sorted list of sites with value labels for every tenth site.

Next we evaluated the docking performance using the enclosure filter (> 0.72) alone and also in combination with the druglike filter (results for the latter are shown in Figure 15). In the SP protocol with GlideScore based ranking of poses the fractions of structures with any, top three and top ranking well-docked poses increased respectively from 55%, 35% and 25% for the whole data set to 65%, 46% and 30% for the closed site subset. They further increased to 74%, 47% and 32% when the druglikeness filter was also applied. Applying Emodel ranking with the same protocol resulted in higher percentages: 65%, 48% and 36% for structures with closed sites and 74%, 51% and 40% for receptors both having closed sites and containing only druglike ligands. Glide Energy based ordering provided similar results to Emodel in regard of the fraction of structures where the top ranking poses had RMSDs lower than 2.0 Å. However, the former afforded a narrower range of structures where the second or third poses were docked within this RMSD limit.

The XP protocol gave again somewhat lower percentages and smaller separations as compared to those of the SP protocol. GlideScore provided the greatest number of well-docked top ranking poses among the three orderings namely 42%, 36% and 29% of docking runs with any, top three and top ranking well-docked poses for the closed site subset and 49%

38% and 33% for closed sites containing druglike ligands. The SP hard docking protocol yielded the highest numbers of successful docking runs in these subsets as well as it had in the druglike subset. In combination with this protocol Emodel based ranking proved to grant the most favorable results: 67%, 54% and 41% of the docking runs to closed sites resulted in at least two well-docked ligands ranked any, top three and top poses. These figures further increased to 75%, 56% and 46% for closed and druglike ligand containing sites, the highest values achieved with the described methodology.

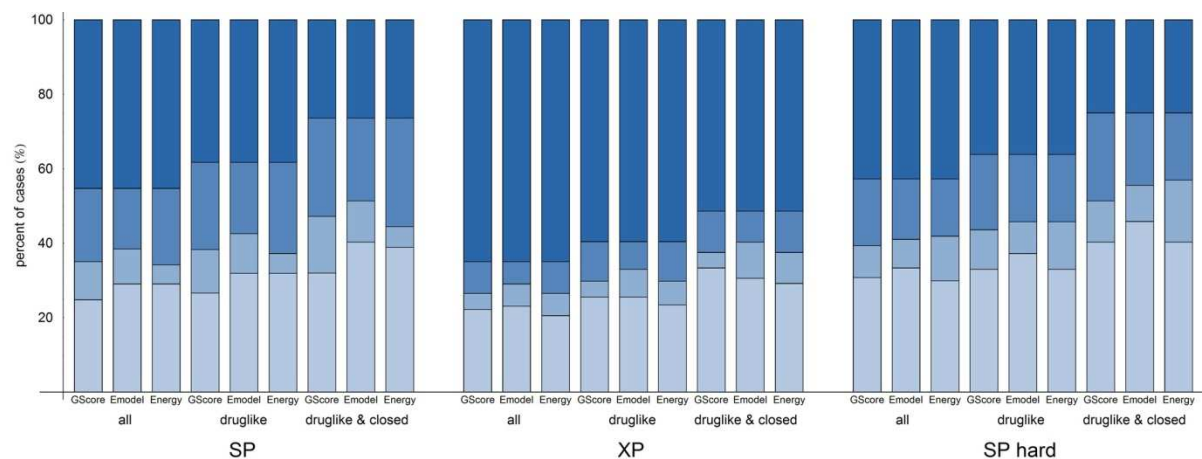


Figure 15. Cumulative fractions of structures with at least two successful consecutive docking steps depending on the docking protocol including precision (SP, XP and SP hard) and pose ranking (GlideScore, Emodel and Glide Energy), and the structure filter (all structures, sites with druglike ligands and closed sites with druglike ligands). From bottom to top: fraction of cases where both of the top ranking poses had RMSD < 2.0 Å (lightest blue), where any of the top three poses had RMSD < 2.0 Å (lightest + light blue), where any of the poses had RMSD < 2.0 Å (lightest + light + mid blue) and all structures in the subset (lightest + light + mid + dark blue). See the appendix for a larger version of the chart.

Discussion

The primary objective of this work was to evaluate the performance of a simple rigid receptor docking methodology in the reproduction of experimental binding modes of ligands in higher stoichiometry protein-ligand complexes, in which binding is supposedly orthosteric. This phenomenon has relevance to fragment based drug discovery in the linking strategy of fragment evolution and to drug-drug interactions as these are frequently mediated by metabolic enzymes or transporters that can bind multiple ligands in their active site. The performance of Glide in docking multiple ligands to their native binding sites was evaluated on a set of 115 protein-ligand complexes from the PDB.

Three different docking settings were tested: default single (SP) and extra precision (XP) and single precision without the scaling of van der Waals radii of ligand atoms (SP hard). Each of them was used in conjunction with two ranking schemes using either GlideScore or Emodel. These two methods disagreed in the selection of the pose to merge with the receptor in only those cases when there was difference in the orders of the top three poses with the two scoring functions, as the top three poses enjoyed priority in the selection process. The finding that the two methods gave qualitatively the same result for most of the docking runs indicated that the docking of the second ligand is not sensitive to small differences in the first ligand's binding mode, which was to be expected. It was also verified that pose ranks were the same for almost all docking steps regardless whether Emodel was utilized for pose selection or the poses from the GlideScore based method were re-ranked by Emodel. Because of this the ranking efficiency of the two scoring functions and also the Glide Energy function could be compared in the three protocols with using only the results from the GlideScore based method. Though excessive differences between the performances of these ranking functions were not discovered, Emodel gave somewhat higher ratios of top ranked well-docked poses than the two other candidates. The single exception was the XP protocol over the subset with closed binding sites and druglike ligands. This shows that Emodel is more accurate than GlideScore SP and even GlideScore XP in ranking the poses in a single docking step. The fractions of structures with at least two well-docked ligands ranked top, which is the optimal scenario when docking compounds with unknown binding modes, were a moderate 29% for the SP protocol, 23% for the XP protocol and 33% for the SP hard protocol. Thus specific subsets of the structures were examined to find criteria for a higher success rate of the method. Among structures featuring sites with SiteMap enclosure values greater than 0.72 and containing druglike ligands ratios of 40%, 33% and 46% were achieved in the SP, XP and SP hard protocols respectively. These are promising results but could still clearly be improved.

More than two ligands could be docked in only a few cases, though the grid size may have been a limitation in this as even the largest possible inner box did not include the centroids of all ligands for some structures. As ligand centroids are allowed to move out of the grid inner box, well-docked poses are possible to find even in these cases but the initial conformations minimized to the well-docked pose may be seriously underrepresented. The highest ratios of successful docking runs are encountered with the SP hard protocol. However, in a cross-docking experiment it cannot be anticipated whether the same behavior will be found since the protein is not a rigid entity and the scaling down of the ligand van der Waals

radii is a rough approximation to take into account small receptor conformational changes. On the other hand, the fact that XP gave the lowest ratios and it rarely produced well-docked poses when SP did not find one either is likely a consequence of its sampling algorithm, which uses specific parts of the molecules from the SP poses as starting cores⁵¹ thus not being able to sample substantially different binding modes from those found by SP.

Further sources of high RMSDs when docking multiple molecules into a large binding site may be the reward and penalty terms of the scoring functions for the filling of hydrophobic pockets by hydrophobic ligand groups or inadequate solvation of groups capable of forming hydrogen bonds. During the first docking step the ligand may partially occupy the space or even important interaction points needed for the binding of the other ligand(s) because those contacts are scored more favorable than those present in the multiply ligated structure. The most common errors in the docking runs identified by inspection of the top poses and experimental binding conformations conform to this hypothesis. In many cases the first docked pose either occupied such specific interaction points of the other ligand or if it was mostly lipophilic it appeared to maximize its contact surface with the receptor. A special case of the latter was when two planar aromatic ligands were aligned parallel in the X-ray structure and the docked poses were also parallel to each other but perpendicular to the experimental binding modes thus the two ligands together filled essentially the same space. Either way the second ligand was partially excluded from the place it should have been docked into, which resulted in misdocked poses and high RMSDs in the docking steps after the first one.

A possible remedy for this problem would be to allow the previously docked ligands to move when docking a new one, which would mean an induced fit approach. However, their use is not so straightforward, since induced fit algorithms are usually implemented to treat only amino acid side chain orientations and not translations and rotations of hetero residues. Furthermore a ligand might need to hop from one interaction point to another involving greater displacement or passing through a higher energy barrier than is usually allowed.

Case Studies

Cytochromes P450

Cytochromes P450 are the most studied promiscuous enzymes and their ability to bind multiple ligands in their active site has been unambiguously demonstrated by X-ray crystallographic studies in several isoforms^{28,30,72-77}. *In vitro* CYP assays are generally used to predict *in vivo* pharmacokinetic properties of drug candidates. However, determination of binding constants is sometimes not straightforward as these assays often show non-Michaelis-Menten kinetic profiles⁸⁻¹⁰ also indicative of cooperative binding of substrates. There is an abounding literature on cooperative binding to CYP3A4⁹ and CYP2C9¹² but similar findings have been published for CYP2A6²⁴, CYP1A2⁷⁸ and the bacterial CYPeryF⁷⁹ as well. Heterotropic cooperativity in these isozymes may lie in the background of drug-drug interactions *in vivo* as well, though only a few studies were able to connect *in vitro* and *in vivo* data directly³²⁻³⁵. Predicting drug-drug interactions or metabolic activation by computational methods is a challenging task since metabolic enzymes usually have broad substrate specificities and heteroactivation profiles are substrate dependent.

Though we aimed at a general investigation of multiple ligand docking, since our data set contained seven cytochrome P450 structures it was straightforward to analyze the performance of the described docking protocol for this pharmaceutically relevant enzyme family. Two further structures were added to this assembly as they fulfilled all but the resolution criterion utilized in the compilation of our data set. These were the structures of human CYP2C8 with two bound retinoic acid residues refined to a resolution of 2.60 Å and human CYP3A4 with two bound ketoconazole molecules with a resolution of 3.80 Å. Thus a set of six bacterial, a rabbit and two human CYP isoforms was obtained. All structure preparation and docking methods were performed for these structures in the same way as for the other members of the data set. Additionally a single precision (SP) docking protocol using Emodel based ranking of poses was performed, in which the top ranking pose was merged with the receptor in every docking step (see representative results of this method in Figure 16).

Selected crystallographic properties and docking results are shown for the nine structures in Table 4. It can be seen that except for the 3g5n structure with three bound ligands of which one is facing the solvent all other CYP sites are characterized by rather high enclosure values. Hence they are categorized as closed ones according to the enclosure criterion employed in

this study (> 0.72). In connection with this calculated site volumes confirm that bacterial CYP isoforms comprise much more compact sites while mammalian CYPs exhibit more spacious ones that can accommodate compounds of various sizes. The ligands present in the bacterial and the rabbit 2B4 isoforms fulfill Lipinski's rules for druglikeness while a logP value of 5.01 was calculated for retinoic acid and ketoconazole has a molecular weight of 531 Da. These compounds are thus not rendered druglike but only by very subtle deviations from the given limits. B-factors of the ligands are also relatively low except for a few cases. These observations permitted the expectation of good docking results.

In the SP and SP hard protocols with Emodel based ranking there was only one docking step that didn't provide any well-docked poses and even that was the third ligand in the triple ligand occupancy structure. The performance of the XP protocol was inferior on this set as it was for the whole data set, only 5 of the 9 docking runs resulted in at least two well-docked ligands. GlideScore allowed only one further unsuccessful docking step in the SP hard and XP protocols but ranks of the poses are higher than with Emodel in many cases. In the SP hard protocol a total of 12 docking steps out of the 19 resulted in well-docked top ranking poses with Emodel and only 9 with GlideScore. This corresponds to 4 (44%) and 2 (22%) out of the 9 structures where two ligands could be docked as top ranking poses for the two scoring functions, respectively. These results for Emodel are encouraging as the 2B4 and 2C8 isoforms were among the cases with two top ranked well-docked ligand poses and the CYP3A4 structure was also well reproduced in the default SP protocol despite the large binding site. The numbers of structures where both poses were among the top three are 6 (67%) for Emodel and 4 (44%) for GlideScore. Thus it seems that this pharmaceutically important enzyme family is a promising target for multiple ligand docking methods.

PDB ID	isoform	res.	encl.	volume	ligands	#	B-fact.	RMSD SP	GS	Em	RMSD XP	GS	Em	RMSD hard	GS	Em
1egy	107	2.35	0.931	489.8	9-aminophenanthrene	1	25.73	0.46	1	1	0.18	2	3	0.20	1	1
						2	35.40	0.37	4	3	1.39	1	1	0.33	1	2
1eup	107	2.10	0.910	615.0	androstenedione	1	29.95	0.57	5	1	0.68	4	4	0.45	5	1
						2	47.27	0.73	1	1	0.62	1	1	0.93	1	1
2whf	130	1.58	0.759	644.8	1-(3-methylphenyl)-1H-benzimidazol-5-amine	1	43.67	0.77	1	2	> 2.00	-	-	0.73	1	2
						2	38.02	0.68	7	5	> 2.00	-	-	> 2.00	-	1
2d0e	158	2.15	0.908	562.5	2-hydroxynaphthoquinone	1	47.45	0.50	6	3	0.76	2	3	0.25	4	12
						2	71.84	0.42	2	1	> 2.00	-	-	0.35	1	1
1t93	158	1.62	0.948	358.1	flaviolin	1	16.50	0.48	3	3	0.48	3	4	0.45	2	2
						2	16.22	0.52	8	9	> 2.00	-	-	0.84	3	8
2z3u	245	2.40	0.905	353.3	chromopyrrolic acid	1	14.79	0.20	1	1	0.20	1	1	0.18	1	1
						2	33.02	0.40	1	1	0.40	1	1	0.34	1	1
3g5n	2B4	2.50	0.672	633.1	1-(biphenyl-4-ylmethyl)-1H-imidazole	1	64.48	0.94	1	1	0.97	1	1	0.94	1	1
						2	40.36	0.61	11	1	> 2.00	-	-	0.41	3	1
						3	73.21	> 2.00	-	-	> 2.00	-	-	> 2.00	-	-
2nnh	2C8	2.60	0.869	772.1	retinoic acid	1	57.23	0.49	1	1	0.39	2	1	0.39	2	1
						2	54.19	0.52	21	14	1.43	1	1	0.49	11	1
2v0m	3A4	3.80	0.808	1247.1	ketoconazole	1	34.35	0.89	1	1	0.93	1	1	1.17	1	1
						2	71.84	1.44	19	2	> 2.00	-	6	1.54	29	30

Table 4. Crystallographic and calculated data and docking results of cytochrome P450 structures. res. = resolution (Å), encl. = enclosure calculated by SiteMap, volume = site volume calculated by SiteMap (Å³), # = ligand number, B-fact. = mean B-factor of the ligand (Å²), RMSDs in the different protocols are given for GlideScore ranking (Å). GS = rank by GlideScore in the protocol with using GlideScore based pose selection, Em = rank by Emodel in the protocol with using Emodel based pose selection.

The aminophenanthrene ligand coordinating the heme iron in the legy structure was perfectly docked as top poses in the SP and SP hard protocols with either GlideScore or Emodel based ranking of poses. In the top pose of the XP protocol the plane of the aromatic rings was flipped though the ligand still occupied about the same space. The second ligand makes apolar contacts with the active site aromatic and aliphatic side chains and its amino group is not involved in any hydrogen bonds in the crystal structure. However, the presence of a hydrogen bond was enforced by the scoring functions in most of the top ranked poses to the hydroxyl group of Tyr75 or to the backbone carbonyl of Phe86, which resulted in a flipped pose, or to two backbone carbonyls of Thr290 and Leu391, which resulted in a totally different binding mode.

The proximal androstenedione in the 1eup structure forms a hydrogen bond with both of its carbonyl groups. One of them is with Asn89 but this was lost in the docking run because the Protein Preparation Wizard flipped the asparagine side chain when optimizing the H-bond network. Presumably this is the reason why GlideScore failed to rank the experimental binding mode as top since when performing the SP docking run with the original side chain orientation even the top ranking pose had an RMSD of 0.44 Å. Many misdocked poses featured a perpendicular orientation of the androstenedione molecule to the heme probably because of electrostatic interactions between the heme iron and one of the carbonyl groups. The distal ligand was well-docked with all docking protocols and scoring functions.

In the 2whf structure the distal binding mode was considered more favorable by GlideScore than the proximal one since it is anchored by two hydrogen bonds involving Thr239 and Asn177. The heme iron coordinated ligand is surrounded mostly by aliphatic side chains and this pocket is not entirely filled, which resulted again in poses with the plane of the benzimidazole core rotated by 180°. Emodel, however, scored the iron coordinating pose to the top thus rendering the well-docked pose second. When docking the proximal ligand after the distal one a pose in which an interligand hydrogen bond is present was favored over the iron coordinated binding mode resulting in the high ranks of the second docking step. When selecting the top poses by Emodel the distal ligand could penetrate deeper into the active site and it did so with its aromatic end retaining only one of its hydrogen bonds and resulting in a high RMSD (see Figure 16). Surprisingly no heme iron coordinating pose could be found with the XP protocol.

The 2d0e and 1t93 structures are of the same CYP isoform and also their co-crystallized ligands are very similar thus the two binding sites are nearly identical. Flaviolin and hydroxynaphthoquinone molecules are capable of forming multiple hydrogen bonds. Active site Arg288 is involved in the anchoring of both ligands in both structures and docked poses but the ligands also exhibit aromatic stacking with the heme and each other. Interestingly this was not preserved in the top ranking poses of the first docking steps instead a binding mode with three hydrogen bonds was found for both compounds. For the second docked flaviolin molecule the stacking interaction was captured well but poses involved in more hydrogen bonds were still enforced for hydroxynaphthoquinone even at the expense of the planarity of its rings.

The two chromopyrrolic acid residues (the natural substrate of CYPStaP) are held very firmly by multiple hydrogen bonds, π - π and cation- π interactions in the 2z3u structure. This also resulted in well-docked top ranked poses in all docking protocols.

The 3g5n structure was one of the cases where the inner grid box did not contain the centroid of all ligands, not even that of the heme iron coordinating inhibitor. In spite of this two molecules were correctly docked in the single precision protocols using Emodel based ranking (see Figure 16). As only the centroid of the semi-distal ligand was contained in the inner box this binding mode was found in the first docking step. It makes contacts mostly with aromatic and aliphatic side chains and the imidazole is encased in a polar environment but is not involved in specific interactions. The iron coordinating binding mode was found second, which was well scored by Emodel but GlideScore ranked a cluster of uncoordinated poses higher in which the methylene group was positioned over the heme iron. Again, it is not known why no iron coordinating pose was found with the XP protocol. This docking run was also performed with the grid centered on only the two ligands closer to the heme but interestingly this did not reverse the order of finding the two different binding modes. The binding conformation of the third ligand, which is partially exposed to the solvent with its imidazole ring, could not be reproduced. Instead poses exhibiting aromatic stacking with the iron coordinating ligand and involved in a hydrogen bond with the amide hydrogen of Gly99 were obtained.

The retinoic acid molecules in the 2nnh structure are both involved in two strong hydrogen bonds with the backbone amides of Gly98 and Ser100 for the proximal and with Asn204 and Arg241 for the distal ligand. These interactions were recovered in all docked

poses and as the ring of the substrate positioned closer to the heme is sterically confined good ranks in the first docking step were acquired. On the other hand flipping of the ring of the distal ligand was encountered in many poses of the second docking step. This produced RMSDs greater than 2.0 Å, though the binding motif is essentially the same (see Figure 16).

The binding conformation of the proximal ketoconazole molecule in the 2v0m structure was remarkably well reproduced with all docking protocols. Even in the second step the acetylpiperazine moiety of the distal ligand was positioned well in the binding site but the positions of the dichlorophenyl and imidazole rings increase the RMSDs (see Figure 16). Important interactions of the distal ligand in the experimental structure are thought to be present between the ligand chlorine atoms and the backbone amide hydrogen of Leu216 and the aromatic ring of Phe213. The imidazole ring of the distal ketoconazole molecule also faces a polar environment. These interactions were replaced by a hydrogen bond between the backbone of Asp217 and the rotated imidazole ring in many of the docked poses, hence high ranks were obtained in the second step.

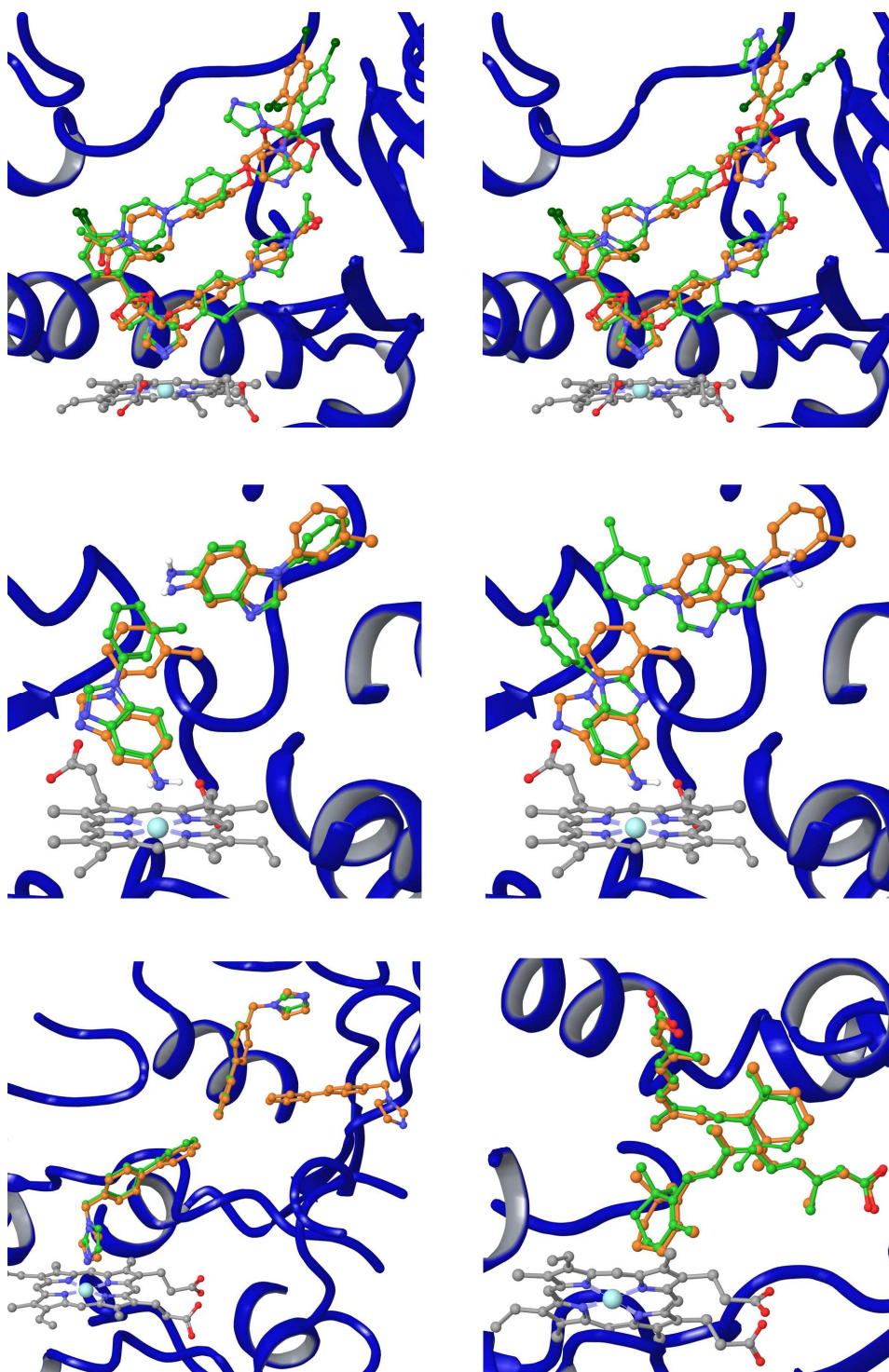


Figure 16. Representative binding modes of ligands in cytochrome P450 complexes obtained with the SP protocol using Emodel based pose ranking. The left column shows the two ligands selected according to their RMSDs as described in the Methods section, the right column shows the results if the top ranking poses were selected in every docking step. The structures from top to bottom are 2v0m, 2whf, bottom left: 3g5n (the results of the two protocols for this structure were identical), bottom right: 2nnh (note the flipped cyclohexene ring of the distal ligand). Heme carbon, docked ligand carbon, docked ligand polar hydrogen, co-crystallized ligand carbon, oxygen, nitrogen, chlorine and iron atoms are colored grey, green, white, orange, red, blue, dark green and cyan respectively.

HSP90 complexes with fragments

Our data set also contained three complexes of the heat shock protein 90-alpha (HSP90) that were known to be the results of fragment screens. This molecular chaperon is a popular target of fragment based drug discovery providing a good example for a successful fragment linking approach³⁸. Each of these complexes contains two different ligands with low B-factors. Binding site of the protein is quite small and enclosure values indicate that it is also closed. Docking results for these structures are shown in Table 5. These results are again encouraging since 2 of the 3 structures were reproduced with the selected poses of both ligands being among the top three using ranking by Emodel in the default SP and SP hard protocols though only the 2qfo structure was reproduced with both of the poses ranked top. The XP protocol provided well-docked poses in both docking steps only for the 2qfo complex. GlideScore based pose ordering gave higher ranks than Emodel in 2 out of the total 10 successful docking steps. The 2xdu complex contained a magnesium ion at a distance of 6.95 Å from one of the ligands, which therefore did not violate our criteria in the compilation of the data set. This nevertheless caused nearly all poses of the pyrimidin-2-amine fragment to be coordinated to the ion thus rendering the whole docking run for this structure unsuccessful. The binding motifs of the fragments in these structures usually comprise only one specific interaction and misdocked poses arise mostly when multiple hydrogen bond donors or acceptors of the receptor are available in the binding site and the alternative position of the fragment does not result in steric clashes when forming a different hydrogen bond. Examples of docking results are shown in Figure 17.

PDB ID	res.	encl.	volume	#	B-fact.	RMSD SP	GS	Em	RMSD XP	GS	Em	RMSD hard	GS	Em
2qfo	1.68	0.761	388.3	1	15.95	0.81	1	1	0.76	1	1	0.83	1	1
				2	17.41	0.42	1	1	0.82	1	1	0.31	1	1
3hz1	2.30	0.795	476.1	1	25.84	0.41	2	3	>2.00	-	-	0.40	6	2
				2	18.53	0.60	3	1	>2.00	-	-	0.71	1	1
2xdu	1.74	0.811	411.9	1	24.60	>2.00	-	-	>2.00	-	-	>2.00	-	-
				2	33.47	>2.00	-	-	>2.00	-	-	>2.00	-	-

Table 5. Crystallographic and calculated data and docking results of structures from HSP90 fragment screens. res. = resolution (Å), encl. = enclosure calculated by SiteMap, volume = site volume calculated by SiteMap (Å³), # = ligand number, B-fact. = mean B-factor of the ligand (Å²), RMSDs in the different protocols are given for GlideScore ranking (Å). GS = rank by GlideScore in the protocol with using GlideScore based pose selection, Em = rank by Emodel in the protocol with using Emodel based pose selection.

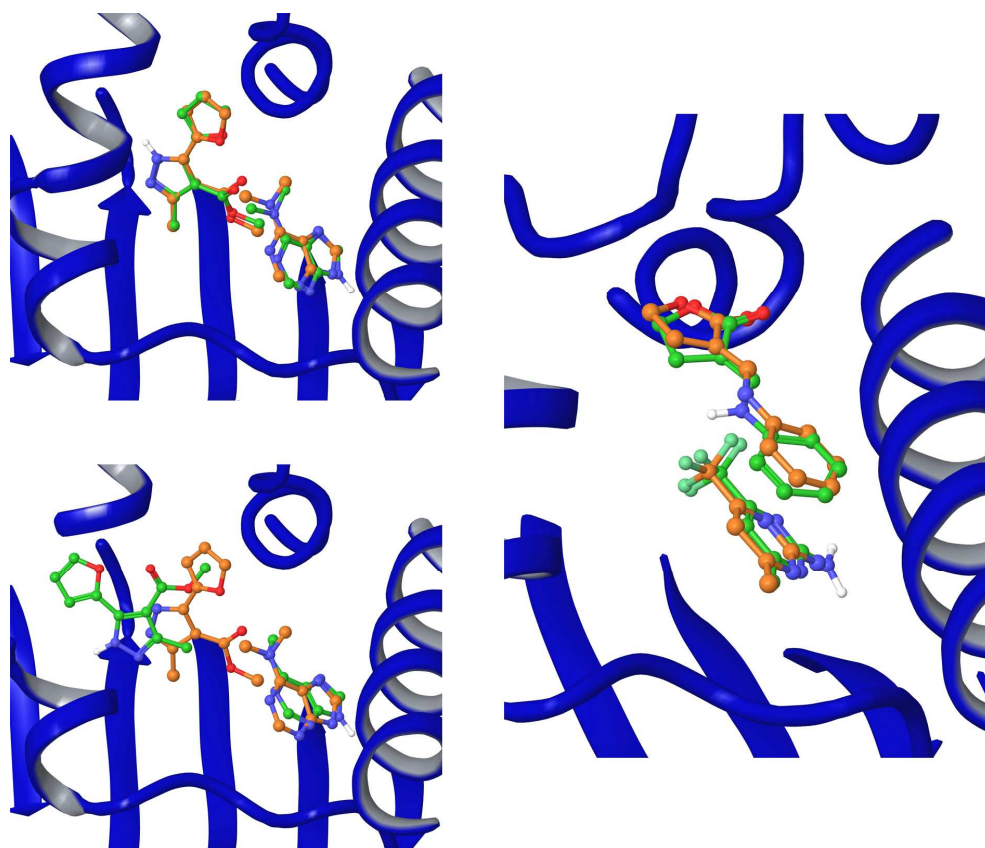


Figure 17. Representative binding modes of ligands in HSP90 complexes obtained with the SP protocol using Emodel based pose ranking. Left top: 3hz1 structure with the two ligands selected according to their RMSDs as described in the Methods section, left bottom: the same structure with the top ranking poses selected in every docking step, right: 2qfo structure, for which the results of the two protocols were identical. Docked ligand carbon, docked ligand polar hydrogen, co-crystallized ligand carbon, oxygen, nitrogen and fluorine atoms are colored green, white, orange, red, blue and turquoise respectively.

Conclusions

The performance of Glide was investigated by using 115 high-resolution protein-ligand complex structures in a sequential docking setup with three different protocols and three different scoring functions. For one third of the whole data set structures with at least two well-docked and top scored ligands were obtained using the SP protocol without the scaling of ligand atom van der Waals radii. The introduction of the druglikeness filter for ligands and closedness filter for binding sites both resulted in higher performance and the ratio of well-reproduced structures increased to 46% for the SP hard protocol when applying both filters. XP was found to provide lower success rates but with a higher probability of the top scoring

poses being well-docked. Three ligands could be docked in only a few cases. Two pharmaceutically relevant small subsets, that of cytochromes P450 and HSP90 complexes from fragment screens, were examined in more detail. Even higher success rates than in the druglike and closed site subset were observed in the former case and also the latter set of structures could be reproduced with the well-docked poses found among the three top ranked ones. These are encouraging results considering the use of large-scale screening applications both in screening for drug-drug interactions and virtual second-site screening in a fragment setup. Efforts, however, are worth to be undertaken using induced fit docking approaches for more precise information on the binding modes of ligands in the case of cooperative binding.

References

- (1) Whitty, A. Cooperativity and biological complexity. *Nat. Chem. Biol.* **2008**, *4*, 435-439.
- (2) Hummel, M. A.; Gannett, P. M.; Aguilar, J. S.; Tracy, T. S. Effector-mediated alteration of substrate orientation in cytochrome P450 2C9. *Biochemistry* **2004**, *43*, 7207-7214.
- (3) Davydov, D. R.; Baas, B. J.; Sligar, S. G.; Halpert, J. R. Allosteric mechanisms in cytochrome P450 3A4 studied by high-pressure spectroscopy: pivotal role of substrate-induced changes in the accessibility and degree of hydration of the heme pocket. *Biochemistry* **2007**, *46*, 7852-7864.
- (4) Locuson, C. W.; Gannett, P. M.; Tracy, T. S. Heteroactivator effects on the coupling and spin state equilibrium of CYP2C9. *Arch. Biochem. Biophys.* **2006**, *449*, 115-129.
- (5) Roberts, A. G.; Campbell, A. P.; Atkins, W. M. The thermodynamic landscape of testosterone binding to cytochrome P450 3A4: ligand binding and spin state equilibria. *Biochemistry* **2005**, *44*, 1353-1366.
- (6) Fishelovitch, D.; Hazan, C.; Hirao, H.; Wolfson, H. J.; Nussinov, R.; Shaik, S. QM/MM study of the active species of the human cytochrome P450 3A4, and the influence thereof of the multiple substrate binding. *J. Phys. Chem. B.* **2007**, *111*, 13822-13832.
- (7) Fishelovitch, D.; Hazan, C.; Shaik, S.; Wolfson, H. J.; Nussinov, R. Structural dynamics of the cooperative binding of organic molecules in the human cytochrome P450 3A4. *J. Am. Chem. Soc.* **2007**, *129*, 1602-1611.
- (8) Hutzler, J. M.; Tracy, T. S. Atypical kinetic profiles in drug metabolism reactions. *Drug Metab. Dispos.* **2002**, *30*, 355-362.
- (9) Houston, J. B.; Galetin, A. Modelling atypical CYP3A4 kinetics: principles and pragmatism. *Arch. Biochem. Biophys.* **2005**, *433*, 351-360.
- (10) Atkins, W. M. Non-Michaelis-Menten kinetics in cytochrome P450-catalyzed reactions. *Annu. Rev. Pharmacol. Toxicol.* **2005**, *45*, 291-310.
- (11) Denisov, I. G.; Frank, D. J.; Sligar, S. G. Cooperative properties of cytochromes P450. *Pharmacol. Ther.* **2009**, *124*, 151-167.
- (12) Zhou, S. F.; Zhou, Z. W.; Yang, L. P.; Cai, J. P. Substrates, inducers, inhibitors and structure-activity relationships of human cytochrome P450 2C9 and implications in drug development. *Curr. Med. Chem.* **2009**, *16*, 3480-3675.
- (13) Guengerich, F. P. Cytochrome P450 and chemical toxicology. *Chem. Res. Toxicol.* **2008**, *21*, 70-83.
- (14) Wong, H.; Tong, V.; Riggs, K. W.; Rurak, D. W.; Abbott, F. S.; Kumar, S. Kinetics of valproic acid glucuronidation: evidence for in vivo autoactivation. *Drug Metab. Dispos.* **2007**, *35*, 1380-1386.
- (15) Uchaipichat, V.; Galetin, A.; Houston, J. B.; Mackenzie, P. I.; Williams, J. A.; Miners, J. O. Kinetic modeling of the interactions between 4-methylumbelliferone, 1-naphthol, and zidovudine

glucuronidation by UDP-glucuronosyltransferase 2B7 (UGT2B7) provides evidence for multiple substrate binding and effector sites. *Mol. Pharmacol.* **2008**, *74*, 1152-1162.

(16) Torres-Rivera, A.; Landa, A. Cooperative kinetics of the recombinant glutathione transferase of *Taenia solium* and characterization of the enzyme. *Arch. Biochem. Biophys.* **2008**, *477*, 372-378.

(17) Martin, C.; Berridge, G.; Higgins, C. F.; Mistry, P.; Charlton, P.; Callaghan, R. Communication between multiple drug binding sites on P-glycoprotein. *Mol. Pharmacol.* **2000**, *58*, 624-632.

(18) Kondratov, R. V.; Komarov, P. G.; Becker, Y.; Ewenson, A.; Gudkov, A. V. Small molecules that dramatically alter multidrug resistance phenotype by modulating the substrate specificity of P-glycoprotein. *Proc. Natl. Acad. Sci. U S A.* **2001**, *98*, 14078-14083.

(19) Higgins, C. F. Multiple molecular mechanisms for multidrug resistance transporters. *Nature.* **2007**, *446*, 749-757.

(20) Sterz, K.; Möllmann, L.; Jacobs, A.; Baumert, D.; Wiese, M. Activators of P-glycoprotein: Structure-activity relationships and investigation of their mode of action. *Chem. Med. Chem.* **2009**, *4*, 1897-1911.

(21) Harlow, G. R.; Halpert, J. R. Analysis of human cytochrome P450 3A4 cooperativity: construction and characterization of a site-directed mutant that displays hyperbolic steroid hydroxylation kinetics. *Proc. Natl. Acad. Sci. U S A.* **1998**, *95*, 6636-6641.

(22) Domanski, T. L.; He, Y. A.; Khan, K. K.; Roussel, F.; Wang, Q.; Halpert, J. R. Phenylalanine and tryptophan scanning mutagenesis of CYP3A4 substrate recognition site residues and effect on substrate oxidation and cooperativity. *Biochemistry* **2001**, *40*, 10150-10160.

(23) Khan, K. K.; He, Y. Q.; Domanski, T. L.; Halpert, J. R. Midazolam oxidation by cytochrome P450 3A4 and active-site mutants: an evaluation of multiple binding sites and of the metabolic pathway that leads to enzyme inactivation. *Mol. Pharmacol.* **2002**, *61*, 495-506.

(24) Harrelson, J. P.; Atkins, W. M.; Nelson, S. D. Multiple-ligand binding in CYP2A6: probing mechanisms of cytochrome P450 cooperativity by assessing substrate dynamics. *Biochemistry* **2008**, *47*, 2978-2988.

(25) Roberts, A. G.; Díaz, M. D.; Lampe, J. N.; Shireman, L. M.; Grinstead, J. S.; Dabrowski, M. J.; Pearson, J. T.; Bowman, M. K.; Atkins, W. M.; Campbell, A. P. NMR studies of ligand binding to P450eryF provides insight into the mechanism of cooperativity. *Biochemistry* **2006**, *45*, 1673-1684.

(26) Cameron, M. D.; Wen, B.; Allen, K. E.; Roberts, A. G.; Schuman, J. T.; Campbell, A. P.; Kunze, K. L.; Nelson, S. D. Cooperative binding of midazolam with testosterone and alpha-naphthoflavone within the CYP3A4 active site: a NMR T1 paramagnetic relaxation study. *Biochemistry* **2005**, *44*, 14143-14151.

(27) Cameron, M. D.; Wen, B.; Roberts, A. G.; Atkins, W. M.; Campbell, A. P.; Nelson, S. D. Cooperative binding of acetaminophen and caffeine within the P450 3A4 active site. *Chem. Res. Toxicol.* **2007**, *20*, 1434-1441.

(28) Schoch, G. A.; Yano, J. K.; Sansen, S.; Dansette, P. M.; Stout, C. D.; Johnson, E. F. Determinants of cytochrome P450 2C8 substrate binding: structures of complexes with montelukast, troglitazone, felodipine, and 9-cis-retinoic acid. *J. Biol. Chem.* **2008**, *283*, 17227-17237.

- (29) Schumacher, M. A.; Miller, M. C.; Brennan, R. G. Structural mechanism of the simultaneous binding of two drugs to a multidrug-binding protein. *EMBO J.* **2004**, *23*, 2923-2930.
- (30) Ekroos, M.; Sjögren, T. Structural basis for ligand promiscuity in cytochrome P450 3A4. *Proc. Natl. Acad. Sci. U S A.* **2006**, *103*, 13682-13687.
- (31) Aller, S. G.; Yu, J.; Ward, A.; Weng, Y.; Chittaboina, S.; Zhuo, R.; Harrell, P. M.; Trinh, Y. T.; Zhang, Q.; Urbatsch, I. L.; Chang, G. Structure of P-glycoprotein reveals a molecular basis for poly-specific drug binding. *Science.* **2009**, *323*, 1718-1722.
- (32) Lasker, J. M.; Huang, M. T.; Conney, A. H. In vitro and in vivo activation of oxidative drug metabolism by flavonoids. *J. Pharmacol. Exp. Ther.* **1984**, *229*, 162-170.
- (33) Tang, W.; Stearns, R. A.; Kwei, G. Y.; Iliff, S. A.; Miller, R. R.; Egan, M. A.; Yu, N. X.; Dean, D. C.; Kumar, S.; Shou, M.; Lin, J. H.; Baillie, T. A. Interaction of diclofenac and quinidine in monkeys: stimulation of diclofenac metabolism. *J. Pharmacol. Exp. Ther.* **1999**, *291*, 1068-1074.
- (34) Hutzler, J. M.; Frye, R. F.; Korzekwa, K. R.; Branch, R. A.; Huang, S. M.; Tracy, T. S. Minimal in vivo activation of CYP2C9-mediated flurbiprofen metabolism by dapsone. *Eur. J. Pharm. Sci.* **2001**, *14*, 47-52.
- (35) Egnell, A. C.; Houston, B.; Boyer, S. In vivo CYP3A4 heteroactivation is a possible mechanism for the drug interaction between felbamate and carbamazepine. *J. Pharmacol. Exp. Ther.* **2003**, *305*, 1251-1262.
- (36) Congreve, M.; Chessari, G.; Tisi, D.; Woodhead, A. J. Recent developments in fragment-based drug discovery. *J. Med. Chem.* **2008**, *51*, 3661-3680.
- (37) Petros, A. M.; Dinges, J.; Augeri, D. J.; Baumeister, S. A.; Betebenner, D. A.; Bures, M. G.; Elmore, S. W.; Hajduk, P. J.; Joseph, M. K.; Landis, S. K.; Nettesheim, D. G.; Rosenberg, S. H.; Shen, W.; Thomas, S.; Wang, X.; Zanze, I.; Zhang, H.; Fesik, S. W. Discovery of a potent inhibitor of the antiapoptotic protein Bcl-xL from NMR and parallel synthesis. *J. Med. Chem.* **2006**, *49*, 656-663.
- (38) Huth, J. R.; Park, C.; Petros, A. M.; Kunzer, A. R.; Wendt, M. D.; Wang, X.; Lynch, C. L.; Mack, J. C.; Swift, K. M.; Judge, R. A.; Chen, J.; Richardson, P. L.; Jin, S.; Tahir, S. K.; Matayoshi, E. D.; Dorwin, S. A.; Lador, U. S.; Severin, J. M.; Walter, K. A.; Bartley, D. M.; Fesik, S. W.; Elmore, S. W.; Hajduk, P. J. Discovery and design of novel HSP90 inhibitors using multiple fragment-based design strategies. *Chem. Biol. Drug. Des.* **2007**, *70*, 1-12.
- (39) Sandor, M.; Kiss, R.; Keseru, G. M. Virtual fragment docking by Glide: a validation study on 190 protein-fragment complexes. *J. Chem. Inf. Model.* **2010**, *50*, 1165-1172.
- (40) Hill, A. V. The possible effects of the aggregation of the molecules of haemoglobin on its dissociation curves. *J. Physiol.* **1910**, *40*, iv-vii.
- (41) Korzekwa, K. R.; Krishnamachary, N.; Shou, M.; Ogai, A.; Parise, R. A.; Rettie, A. E.; Gonzalez, F. J.; Tracy, T. S. Evaluation of atypical cytochrome P450 kinetics with two-substrate models: evidence that multiple substrates can simultaneously bind to cytochrome P450 active sites. *Biochemistry* **1998**, *37*, 4137-4147.
- (42) Galetin, A.; Clarke, S. E.; Houston, J. B. Quinidine and haloperidol as modifiers of CYP3A4 activity: multisite kinetic model approach. *Drug Metab. Dispos.* **2002**, *30*, 1512-1522.

- (43) Qu, Q.; Sharom, F. J. Proximity of bound Hoechst 33342 to the ATPase catalytic sites places the drug binding site of P-glycoprotein within the cytoplasmic membrane leaflet. *Biochemistry* **2002**, *41*, 4744-4752.
- (44) Lugo, M. R.; Sharom, F. J. Interaction of LDS-751 with P-Glycoprotein and mapping of the location of the R drug binding site. *Biochemistry* **2005**, *44*, 643-655.
- (45) Egnell, A. C.; Eriksson, C.; Albertson, N.; Houston, B.; Boyer, S. Generation and evaluation of a CYP2C9 heteroactivation pharmacophore. *J. Pharmacol. Exp. Ther.* **2003**, *307*, 878-887.
- (46) Egnell, A. C.; Houston, J. B.; Boyer, C. S. Predictive models of CYP3A4 Heteroactivation: in vitro-in vivo scaling and pharmacophore modeling. *J. Pharmacol. Exp. Ther.* **2005**, *312*, 926-937.
- (47) Wester, M. R.; Yano, J. K.; Schoch, G. A.; Yang, C.; Griffin, K. J. The structure of human cytochrome P450 2C9 complexed with flurbiprofen at 2.0-Å resolution. *J. Biol. Chem.* **2004**, *279*, 35630-35637.
- (48) Williams, P. A.; Cosme, J.; Ward, A.; Angove, H. C.; Matak Vinković, D.; Jhoti, H. Crystal structure of human cytochrome P450 2C9 with bound warfarin. *Nature*, **2003**, *424*, 464-468.
- (49) Locuson, C. W.; Gannett, P. M.; Ayscue, R.; Tracy, T. S. Use of simple docking methods to screen a virtual library for heteroactivators of cytochrome P450 2C9. *J. Med. Chem.* **2007**, *50*, 1158-1165.
- (50) Kapelyukh, Y.; Paine, M. J. I.; Maréchal, J.-D.; Sutcliffe, M. J.; Wolf, C. R.; Roberts, G. C. K. Multiple substrate binding by cytochrome P450 3A4: estimation of the number of bound substrate molecules. *Drug Metab. Dispos.* **2008**, *36*, 2136-2144.
- (51) Kitchen, D. B.; Decornez, H.; Furr, J. R.; Bajorath, J. Docking and scoring in virtual screening for drug discovery: methods and applications. *Nat. Rev. Drug. Discov.* **2004**, *3*, 935-949.
- (52) Mohan, V.; Gibbs, A. C.; Cummings, M. D.; Jaeger, E. P.; DesJarlais, R. L. Docking: successes and challenges. *Curr. Pharm. Des.* **2005**, *11*, 323-333.
- (53) Leach, A. R.; Shoichet, B. K.; Peishoff, C. E. Prediction of protein-ligand interactions. Docking and scoring: successes and gaps. *J. Med. Chem.* **2006**, *49*, 5851-5855.
- (54) Kroemer, R. T. Structure-based drug design: docking and scoring. *Curr. Protein Pept. Sci.* **2007**, *8*, 312-328.
- (55) Warren, G. L.; Andrews, C. W.; Capelli, A. M.; Clarke, B.; LaLonde, J.; Lambert, M. H.; Lindvall, M.; Nevins, N.; Semus, S. F.; Senger, S.; Tedesco, G.; Wall, I. D.; Woolven, J. M.; Peishoff, C. E.; Head, M. S. A critical assessment of docking programs and scoring functions. *J. Med. Chem.* **2006**, *49*, 5912-5931.
- (56) Kontoyianni, M.; McClellan, L. M.; Sokol, G. S. Evaluation of docking performance: comparative data on docking algorithms. *J. Med. Chem.* **2004**, *47*, 558-565.
- (57) Cummings, M. D.; DesJarlais, R. L.; Gibbs, A. C.; Mohan, V.; Jaeger, E. P. Comparison of automated docking programs as virtual screening tools. *J. Med. Chem.* **2005**, *48*, 962-976.

- (58) Cross, J. B.; Thompson, D. C.; Rai, B. K.; Baber, J. C.; Fan, K. Y.; Hu, Y.; Humblet, C. Comparison of several molecular docking programs: pose prediction and virtual screening accuracy. *J. Chem. Inf. Model.* **2009**, *49*, 1455-1474.
- (59) McGann, M. FRED pose prediction and virtual screening accuracy. *J. Chem. Inf. Model.* **2011**, *51*, 578-596.
- (60) Schrödinger Suite 2010 Protein Preparation Wizard; Epik version 2.1, Schrödinger, LLC, New York, NY, 2010; Impact version 5.6, Schrödinger, LLC, New York, NY, 2010; Prime version 2.2, Schrödinger, LLC, New York, NY, 2010.
- (61) Molecule File Converter, version 5.4.1.1, © 1999-2011 ChemAxon Ltd.
- (62) LigPrep, version 2.4, Schrödinger, LLC, New York, NY, 2010.
- (63) Epik, version 2.1, Schrödinger, LLC, New York, NY, 2010.
- (64) Shelley, J. C.; Cholleti, A.; Frye, L. L.; Greenwood, J. R.; Timlin, M. R.; Uchiyama, M. Epik: a software program for pKa prediction and protonation state generation for druglike molecules. *J. Comput. Aided Mol. Des.*, **2007**, *21*, 681-691.
- (65) Greenwood, J. R.; Calkins, D.; Sullivan, A. P.; Shelley, J. C. Towards the comprehensive, rapid, and accurate prediction of the favorable tautomeric states of drug-like molecules in aqueous solution. *J. Comput. Aided Mol. Des.*, **2010**, *24*, 591-604.
- (66) Calculator, version 5.4.1.1, © 1998-2011 ChemAxon Ltd.
- (67) SiteMap, version 2.4, Schrödinger, LLC, New York, NY, 2010.
- (68) Glide, version 5.6, Schrödinger, LLC, New York, NY, 2010.
- (69) Friesner, R. A.; Banks, J. L.; Murphy, R. B.; Halgren, T. A.; Klicic, J. J.; Mainz, D. T.; Repasky, M. P.; Knoll, E. H.; Shelley, M.; Perry, J. K.; Shaw, D. E.; Francis, P.; Shenkin, P. S. Glide: a new approach for rapid, accurate docking and scoring. 1. Method and assessment of docking accuracy. *J. Med. Chem.* **2004**, *47*, 1739-1749.
- (70) Halgren, T. A.; Murphy, R. B.; Friesner, R. A.; Beard, H. S.; Frye, L. L.; Pollard, W. T.; Banks, J. L. Glide: a new approach for rapid, accurate docking and scoring. 2. Enrichment factors in database screening. *J. Med. Chem.* **2004**, *47*, 1750-1759.
- (71) Friesner, R. A.; Murphy, R. B.; Repasky, M. P.; Frye, L. L.; Greenwood, J. R.; Halgren, T. A.; Sanschagrin, P. C.; Mainz, D. T. Extra precision Glide: docking and scoring incorporating a model of hydrophobic enclosure for protein-ligand complexes. *J. Med. Chem.* **2006**, *49*, 6177-6196.
- (72) Cupp-Vickery, J.; Anderson, R.; Hatziris, Z. Crystal structures of ligand complexes of P450eryF exhibiting homotropic cooperativity. *Proc. Natl. Acad. Sci. U S A.* **2000**, *97*, 3050-3055.
- (73) Podust, L. M.; Ouellet, H.; von Kries, J. P.; de Montellano, P. R. Interaction of Mycobacterium tuberculosis CYP130 with heterocyclic arylamines. *J. Biol. Chem.* **2009**, *284*, 25211-25219.
- (74) Zhao, B.; Guengerich, F. P.; Voehler, M.; Waterman, M. R. Role of active site water molecules and substrate hydroxyl groups in oxygen activation by cytochrome P450 158A2: a new mechanism of proton transfer. *J. Biol. Chem.* **2005**, *280*, 42188-42197.

- (75) Zhao, B.; Guengerich, F. P.; Bellamine, A.; Lamb, D. C.; Izumikawa, M.; Lei, L.; Podust, L. M.; Sundaramoorthy, M.; Kalaitzis, J. A.; Reddy, L. M.; Kelly, S. L.; Moore, B. S.; Stec, D.; Voehler, M.; Falck, J. R.; Shimada, T.; Waterman, M. R. Binding of two flavin substrate molecules, oxidative coupling, and crystal structure of *Streptomyces coelicolor* A3(2) cytochrome P450 158A2. *J. Biol. Chem.* **2005**, *280*, 11599-11607.
- (76) Makino, M.; Sugimoto, H.; Shiro, Y.; Asamizu, S.; Onaka, H.; Nagano, S. Crystal structures and catalytic mechanism of cytochrome P450 StaP that produces the indolocarbazole skeleton. *Proc. Natl. Acad. Sci. U S A.* **2007**, *104*, 11591-11596.
- (77) Gay, S. C.; Sun, L.; Maekawa, K.; Halpert, J. R.; Stout, C. D. Crystal structures of cytochrome P450 2B4 in complex with the inhibitor 1-biphenyl-4-methyl-1H-imidazole: ligand induced structural response through α -helical repositioning. *Biochemistry* **2009**, *48*, 4762-4771.
- (78) Sohl, C. D.; Isin, E. M.; Eoff, R. L.; Marsch, G. A.; Stec, D. F.; Guengerich, F. P. Cooperativity in oxidation reactions catalyzed by cytochrome P450 1A2: highly cooperative pyrene hydroxylation and multiphasic kinetics of ligand binding. *J. Biol. Chem.* **2008**, *283*, 7293-7308.
- (79) Khan, K. K.; Liu, H.; Halpert, J. R. Homotropic versus heterotopic cooperativity of cytochrome P450eryF: a substrate oxidation and spectral titration study. *Drug Metab. Dispos.* **2003**, *31*, 356-359.

Appendix

PDB ID codes and chain identifiers of the structures used in the study:

structures containing 2 similar ligands:

1dog/A, 1e7c/A, 1eb9/AB, 1egy/A, 1eup/A, 1fm4/A, 1gnw/AB, 1hkk/A, 1k0y/ABCD, 1l5q/AB, 1oni/ABC, 1pzo/A, 1qiw/A, 1rb3/AB, 1rxj/ABCD, 1t93/A, 1tcw/AB, 1tw4/A, 1txc/AB, 1v08/AB, 1z62/A+mate, 1znd/A, 2ayw/A, 2b99/ABCDE, 2bjw/A, 2cbo/A, 2cbt/AB, 2cmw/A, 2d0e/A, 2d41/A, 2e93/AB, 2e9a/AB, 2e9c/AB, 2flh/D, 2ft9/A, 2g8r/A, 2hfp/AB, 2iei/AB, 2nss/A, 2nvd/A, 2oz5/A, 2p70/A, 2uxi/AB, 2wbb/ABCD, 2wbd/ABCD, 2whf/A, 2whh/A, 2wrm/A, 2x0v/B, 2xuc/A, 2z3u/A, 2z4y/AB, 2zeb/ABCD, 2zf4/AB, 3a73/A, 3b6c/AB, 3bc4/A+mate, 3bxs/AB, 3cr4/X, 3cz0/AB, 3cz1/AB, 3dzt/AB, 3e3u/A, 3e7s/AB, 3etd/ABCDEF, 3etg/ABCDEF, 3f3t/A, 3f3u/A, 3g35/B, 3g35/B, 3g6m/A, 3gqt/ABCD, 3h78/AB, 3hlw/A, 3htf/A, 3huo/A, 3ilt/BE, 3km4/A, 3ko0/AB, 3krq/A, 3ljb/E, 3lc3/AB, 3os9/ABCD

structures containing 2 different ligands:

1me7/A+mate, 1s9q/AB+2mates, 1u30/A, 2aov/A, 2qfo/A, 2vq5/AB, 2wk2/A, 2xdu/A, 3hz1/A, 3iiq/A, 3jun/AB

structures containing 3 ligands:

1dtl/A, 1e7c/A, 1lin/A, 1n8v/A, 2a3b/A, 2d5z/ABCD, 2e99/AB, 2hdu/B, 2qd3/AB, 3b99/A, 3dhh/ABCE, 3ej0/A+3mates, 3g5n/D, 3p2r/AB

structures containing 4 ligands:

1wrk/AB, 2a3a/A, 2e98/AB, 2fsz/AB+2mates, 2qim/A, 3e85/A, 3em0/A

structures containing 5 ligands:

3elz/A

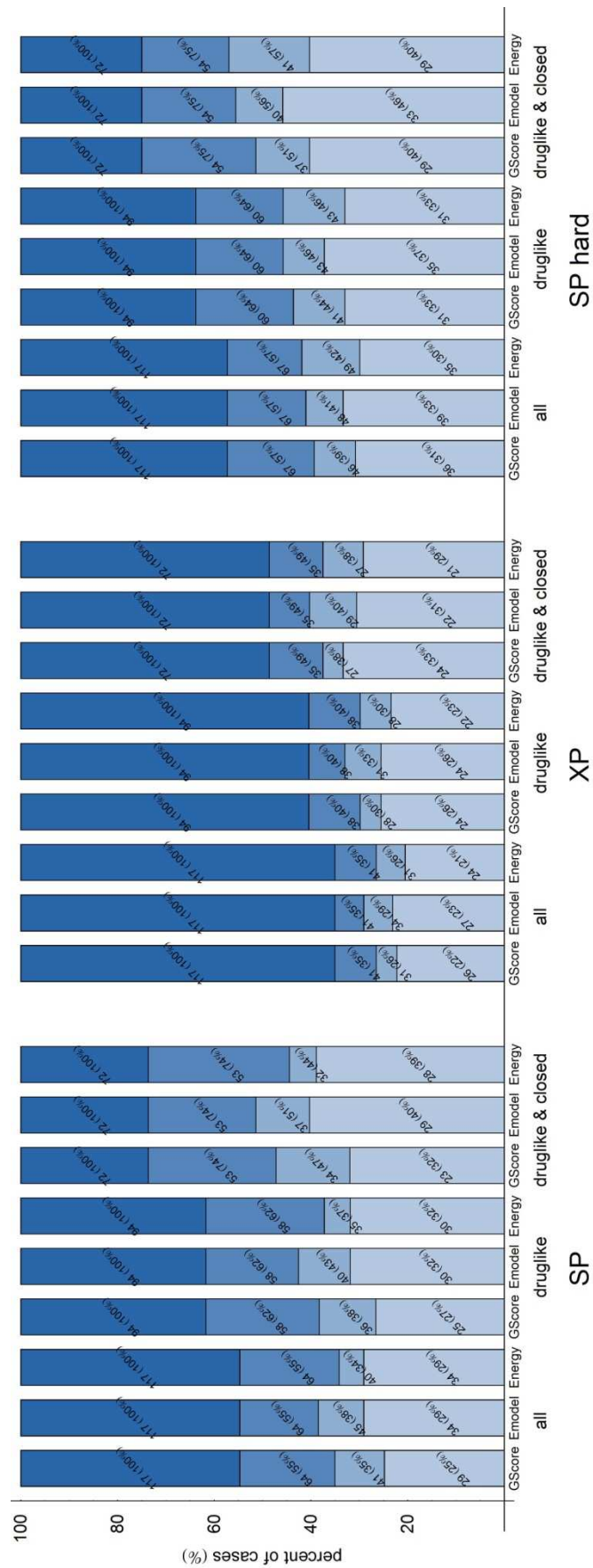
structures containing 6 ligands:

3lsl/AD

the two structures added in the CYP case study:

2nnh/A, 2v0m/A

Figure 15 with percentages indicated:



Summary

In the case of proteins involved in drug metabolism and transport non-Michaelis-Menten kinetic profiles are often observed, which is indicative of the cooperative binding of multiple drug molecules to these enzymes. The presence of auto- and heteroactivation can increase *in vivo* metabolic rates and the alteration in transport can change the distribution of drugs among tissues in the body. These phenomena may result in failure of drug candidates in late phases of drug development or undesirable drug-drug interactions. Therefore early prediction of them using computational methods would mean an important achievement. However, only a few models developed for limited diversity ligand sets can be found in the literature, comprehensive studies on the prediction of cooperative ligand binding have not been reported.

In this work we aimed at the modeling of cooperative binding using molecular docking not only among metabolic enzymes but on a general test set of protein-ligand complexes. To this ends structures from the RCSB Protein Data Bank (PDB) with at least 2.5 Å resolution and containing a ligand cluster of 2-6 ligands in close proximity to each other were compiled with a script. The performance of Glide, a docking program developed by Schrödinger, was evaluated on the obtained set of 115 complexes with respect to structure reproduction. A sequential docking protocol was used throughout the work, in which either the first well-docked pose or the pose with the least RMSD from any experimental ligand conformation was merged with the protein structure in each step and the resulting complex were carried on to the further docking steps. The program was tested using three different settings (single precision – SP, extra precision – XP, single precision without the scaling of ligand atom van der Waals radii – SP hard) and three different scoring functions (GlideScore, Emodel, Glide Energy).

For one third of the whole data set structures with at least two well-docked and top scored ligands were obtained using the SP protocol without the scaling of ligand atom van der Waals radii. The introduction of the druglikeness filter for ligands and closedness filter for binding sites both resulted in higher performance and the ratio of well-reproduced structures increased to 46% for the SP hard protocol when applying both filters. XP was found to provide lower success rates but with a higher probability of the top scoring poses being well-docked. Three ligands could be docked in only a few cases. Two pharmaceutically relevant small subsets, that of cytochromes P450 and HSP90 complexes from fragment screens, were examined in more detail. Even higher success rates than in the druglike and closed site subset were observed in the former case and also two of the latter set of structures could be reproduced with the well-docked poses found among the three top ranked ones.

These are encouraging results considering the use of large-scale screening applications both in screening for drug-drug interactions and virtual second-site screening in a fragment setup. Efforts, however, are worth to be undertaken using for example induced fit docking approaches for more precise information on the binding modes of ligands in the case of cooperative binding.

Összefoglalás

A gyógyszerek metabolizmusában és transzportjában részt vevő fehérjék esetén kinetikai méréseknél gyakran tapasztalható a klasszikus Michaelis-Menten modelltől eltérő viselkedés, mely egyszerre több gyógyszermolekula kooperatív kötődését jelzi ezen enzimekhez. Auto- illetve heteroaktiváció fellépése jelentősen megnövelheti a gyógyszer szerkezetbeli lebontásának sebességét, a transzportfolyamatok megváltozása pedig a szövetek közötti disztribúciót befolyásolhatja. Ezen jelenségek a gyógyszerfejlesztés késői szakaszában való elbukást illetve nemkívánatos gyógyszerkölsönhatásokat eredményezhetnek, így számítógépes módszerekkel történő korai előrejelzésük igen fontos eredmény lenne. Mindazonáltal az irodalomban csak néhány, specifikus ligandumkészletre kialakított modell található, a jelenség átfogó tanulmányozására számítógépes módszerek felhasználásával nincs példa.

Munkámban a kooperatív kötődés jelenségének molekuláris dokkolással történő modellezését nem csak a metabolikus enzimek körében, hanem általánosan tűztem ki. Ennek érdekében az RCSB Fehérje Adatbázisból (PDB) automatizált módon azon legalább 2.5 Å felbontású fehérje szerkezeteket kerestem ki, melyekben található legalább egy 2-6 egymáshoz közeli ligandumot tartalmazó ligandum klaszter. A kapott 115 komplex esetén a Schrödinger által fejlesztett Glide dokkoló program teljesítményét vizsgáltam a ligandumok kísérletileg meghatározott kötő konformációi reprodukciójának szempontjából. A munka során egy szekvenciális dokkolási protokollt alkalmaztam, melynek minden lépésében a legalacsonyabb sorszámú sikeres vagy a kristálybeli ligandumoktól való legkisebb RMSD eltérésű dokkolt konformációt egyesítettem a fehérjeszerkezettel, és a kapott komplexbe történtek a további dokkolások. A programot három különböző beállítással (normál pontosság – SP, extra pontosság – XP, ligandum atomsugár skálázás nélküli normál pontosság – kemény SP) és három különböző pontozófüggvény (GlideScore, Emodel, Glide Energy) használatával teszteltem.

Az adatkészlet egyharmadánál a kemény SP beállítással és az Emodel pontozófüggvény használatával sikerült legalább két ligandum kötő konformációját első pózként reprodukálni. A gyógyszeryszerű ligandumokat tartalmazó és zárt kötőhelyű komplexek által alkotott részhalmazban az ilyen sikeres dokkolások aránya hasonló beállításokkal 46%-ra nőtt. Az XP módszer ennél alacsonyabb sikeres dokkolási arányt mutatott, azonban ott az első dokkolt pózok nagyobb valószínűséggel jelentettek sikeres dokkolást. Három ligandum kötő konformációjának reprodukálása csak néhány esetben sikerült. Két, a gyógyszerkutatás szempontjából lényeges kisebb részhalmazt is megvizsgáltam, ezek a citokróm P450 metabolikus enzimek és a HSP90 chaperon fragmensekkel alkotott komplexei voltak. Az előbbieken esetén még magasabb sikeres dokkolási arány mutatkozott, és az utóbbiaknál is sikerült két komplex szerkezetét reprodukálni az első három dokkolt pózok között.

Ezek a virtuális szűrésben alkalmazható módszerek pontosságát tekintve biztató eredmények, mindazonáltal további erőfeszítések szükségesek például az indukált illeszkedésen alapuló dokkolási módszerek (IFD) ligandumokra történő kiterjesztése által, kooperatívan kötődő ligandumok kísérleti kötő konformációinak pontosabb előrejelzése érdekében.